

**DEVELOPMENT OF CAPABILITIES OF OPTICAL DIFFRACTION
ANALYSIS FOR QUANTITATIVELY COMPARING AND
CORRELATING ROCK FABRICS AND FABRIC CHANGES**

AD 73390

Annual Technical Report
(Jan. 11, 1971 - Jan. 10, 1972)

Reproduced by
**NATIONAL TECHNICAL
INFORMATION SERVICE**
Springfield, Va. 22151

DDC
RECEIVED
FEB 29 1972
RECEIVED
B

DISTRIBUTION STATEMENT A

Approved for public release;
Distribution Unlimited



Sponsored by:

Advanced Research Projects Agency
ARPA Order No. 1579, Amend. No. 2
Program Code No. 1F10

Monitored by:

U.S. Bureau of Mines

Prepared by:

Professor Howard J. Pincus
Principal Investigator
The University of Wisconsin—Milwaukee
February 10, 1972

THIS IS A SPECIAL COPY CONTAINING A
SET OF ORIGINAL PRINTS OF PHOTOGRAPHS.

48

DISCLAIMER NOTICE

THIS DOCUMENT IS THE BEST
QUALITY AVAILABLE.

COPY FURNISHED CONTAINED
A SIGNIFICANT NUMBER OF
PAGES WHICH DO NOT
REPRODUCE LEGIBLY.

Mar 7, 66

UNCLASSIFIED

Security Classification

DOCUMENT CONTROL DATA - I & D

(Security Classification of title, text, tables, and indexes must be entered when the report is classified)

1. ORIGINATING AGENCY (Name of agency or organization) UNIVERSITY OF WISCONSIN	2. REPORT SECURITY CLASSIFICATION UNCLASSIFIED 3. GROUP
--	--

3. REPORT TITLE
DEVELOPMENT OF CAPABILITIES OF OPTICAL DIFFRACTION ANALYSIS FOR QUANTITATIVELY COMPARING AND CORRELATING ROCK FABRICS AND FABRIC CHANGES

4. DESCRIPTIVE NOTES (Type of report, inclusive dates)
FIRST ANNUAL TECHNICAL REPORT, JAN. 11, 1971 - JAN. 10, 1972

5. AUTHOR(S) (Full name, title, organization)
**PROF. HOWARD J. PERCIE
DEPT. OF GEOLOGICAL SCIENCES
UNIVERSITY OF WISCONSIN-MILWAUKEE**

6. REPORT DATE FEBRUARY 10, 1972	7a. TOTAL NO. OF PAGES 89	7b. NO. OF PAGES 89 (Appendix B)
--	-------------------------------------	--

8a. CONTRACT OR GRANT NO. H021003	9a. ORIGINATOR'S REPORT NUMBER(S) ANNUAL TECHNICAL REPORT #1 (Acct. 144B567)
b. PROJECT NO. ARMA CENTER 1579, AGENCY NO. PROGRAM CODE NO.	9b. OTHER REPORT NO(S) (Any other numbers that may be assigned this report)
c.	
d.	

10. DISTRIBUTION STATEMENT
DISTRIBUTION OF THIS DOCUMENT IS UNLIMITED.

11. SUPPLEMENTARY NOTES	12. SPONSORING/MONITORING AGENCY NAME(S) AND ADDRESS(ES) Director Advanced Research Projects Agency Washington, D. C. 20301 Att: Program Mgmt.
-------------------------	--

13. ABSTRACT

Photographs and acetate peels of rock specimens undergoing deformation have been converted to their two-dimensional Fourier amplitude transforms by optical diffraction. Changes in the transforms reflect spatial changes in the rock fabrics. Maps of the transforms assist in their interpretation. Transforms have also been produced using partially coherent light and a modified microscope system.

Suites of spatial filters produced from theoretical considerations and modified transforms have been constructed for differential analysis of the spatial frequency content of input photographs.

Holographic subtraction of one test input from another has been started, laying the foundation for another approach to mapping fabric changes in progressive deformation.

UNCLASSIFIED

3200.8 (Att 1 to Encl 1)
Mar 7, 66

Security Classification

14 KEY WORDS	LINK A		LINK B		LINK C	
	ROLE	WT	ROLE	WT	ROLE	WT
Optical diffraction analysis	8	3				
Rock fabrics	7	3				
Rock deformation	6	2				
Maps of Fourier transforms	10	3				
Fourier transform visible through microscope eyepiece	10	1				
Differential analysis of spatial frequency content			10	0		
Holographic subtraction					10	0

UNCLASSIFIED

Security Classification

DEVELOPMENT OF CAPABILITIES OF OPTICAL
DIFFRACTION ANALYSIS FOR QUANTITATIVELY
COMPARING AND CORRELATING ROCK FABRICS
AND FABRIC CHANGES

Annual Technical Report (First year, Jan. 11, 1971 - Jan. 10, 1972)
Report due Feb. 11, 1972

ARPA ORDER NO. 1579 Amend. No. 2
Program Code No. 1F10

Monitored by U. S. Bureau of Mines
Contract No. H0210003

CONTRACTOR - UNIVERSITY OF WISCONSIN
(U. W. Acct. No. 144-B567)

Principal Investigator:
Professor H. J. Pincus
Dept. of Geological Sciences
University of Wisconsin-Milwaukee
Milwaukee, Wisconsin 53201
Tel. (414) 963-4441
-4017

Effective date of contract:
January 11, 1971

Contract Expiration date:
January 11, 1972 (End of first year
of three-year project)

Project Engineer:
Mr. Robert C. Steckley
Twin Cities Mining Research Center
P. O. Box 1660
Twin Cities, Minnesota 55111
Tel. (612) 725-4567

Amount of contract:
\$35,225 for first year

Sponsored by:
Advanced Research Projects Agency
ARPA Order No. 1579, Amend. No. 2
Program Code No. 1F10

Disclaimer: The views and conclusions contained in this document are those of the author and should not be interpreted as necessarily representing the official policies, either express or implied, of the Advanced Research Projects Agency or the U. S. Government.

Note: This annual technical report is submitted in compliance with Sec. 2.8, p. 6 and Data and Reporting Clause, para. (b) (1) (ii), pp. 13, 14 of the contract.

**Details of illustrations in
this document may be better
studied on microfilm**

Prepared by:


Feb. 10, 1972
Professor Howard J. Pincus
Principal Investigator

TABLE OF CONTENTS

	<u>Page</u>
List of Illustrations	i
Technical Report Summary	iv
Abstract (see Appendix E)	E-1, item #13
1. Introduction	1
1.1 Purpose and objectives of the project	1
1.2 Background	2
1.3 Assumptions and limitations	3
1.4 Acknowledgments	4
2. Methods of Analysis	5
2.1 Introduction	5
2.2 Optical analysis	5
2.3 Rock deformation experiments	10
2.4 Ancillary analyses and developments	11
3. Important Analytical Developments	13
4. Technical Problems Encountered	15
5. Results to Date	18
6. Implications for Further Research	21

(continued)

Table of Contents (continued)	<u>page</u>
7. Special Comments	22
8. Concluding Remarks	22
Appendixes	
A - Figures Accompanying Text	A-1 - 26
B - List of References Consulted	B-1 - 5
C - Outlines of Procedures	C-1 - 22
D - Distribution List	D-1 - 4
E - Form DD 1473 (Abstract)	E-1, 2

LIST OF ILLUSTRATIONS

	<u>page</u>
Figure 1 - Schematic diagram for optical diffraction analysis. The two products are the transform (spectrum) and the filtered output.	A-1
Figure 2 - Young's double-slit experiment. $y_1 B_0$ (or y_1) varies with spatial frequency ($1/s$) in the input plane.	A-2
Figure 3 - Fraunhofer diffraction with a lens. y in the transform plane varies with $1/s$ in the input plane.	A-3
Figure 4 - Fourier transform relationships in a single lens system.	A-4
Figure 5 - some Fourier transform pairs, (a)-(h).	A-5
Figure 6 - Portion of rock mechanics laboratory. From left to right: a) uniaxial set-up (details in Figure 8); b) electrical hardware for strain gage work (details in Figure 12); c) rock slice set-up (details in Figure 10); d) third-part loading set-up; e) biaxial set-up.	A-6
Figure 7 - Rock drill used for preparing cylindrical specimens. NX thin-walled bit shown cutting core from large concrete test cylinder. Base clamp is designed to hold irregular specimens.	A-7
Figure 8 - Uniaxial set-up with photographic equipment for recording surface fabric during loading.	A-8
Figure 9 - Sample test results from uniaxial loading as shown in Figure 8.	A-9
Figure 10 - Rock slice set-up, cantilever loading. Rock slice is cemented to loaded aluminum beam. Slice and beam to right support dummy gage for temperature compensation. Photographic equipment above slice records surface fabric during loading.	A-10
Figure 11 - Strain gage circuitry for rock slice test using the cantilever loading assembly.	A-11
Figure 12 - Electrical hardware for strain gage work. From left to right: indicator unit, stacked switching and balancing units, quick-connect junction box.	A-12
Figure 13 - Sample test results from cantilever loading as shown in Figure 10, using instrumentation of Figures 11 and 12.	A-13

Figure 14 - Figure 14 - Configurations of components on the optical bench for producing holographic transforms.

a) Rayleigh configuration. A small lens at position i generates a point source of light in the input plane ii. The holographic transform is recorded at iii.

A-14

b) Mach-Zender configuration. Beam splitters are at i, the input at ii, and the holographic transform is recorded at iii. This configuration will produce holographic reconstructed images if the second beam splitter-mirror assembly is positioned beyond the reconstruction objectives iv.

A-15

Figure 15 - A diagrammatic representation of the reversal development process. From Neward, 1971.

A-16

Figure 16 - Photographs of a slice of Barre granite (face 2) undergoing cantilever deformation. Magnification = 2.5x. Load on the cantilever is to the right. The pictures a, b, c correspond to the points A1, A5, A9 on the curve in Figure 17.

A-17

Figure 17 - Loading curve for the deformation series illustrated in Figure 16.

A-18

Figure 18 - Transforms of inputs in Figure 17. b) and c) are almost identical and show less high frequency content than a).

A-19

Figure 19 - Maps of the transforms illustrated in Figure 18. There is more low frequency content in b) and c) than in a). c) appears to be more uniform than b) in diffraction elements.

A-20

Figure 20 - Acetate peels made during deformation of a slice of Barre granite, face 13. Load on the cantilever is toward the top of the pictures. Magnification = 4.4x. Inputs were masked to cover same area in each. a) b) and c) correspond to the points a, c, and g, respectively in Figure 21. Some fractures in a) appear to have widened and/or extended in b). New fractures appear in both b) and c). Some of those appearing in b) are longer in c).

A-21

Figure 21 - Loading curve for the deformation series illustrated in Figure 20.

A-22

Figure 22 - Transforms corresponding to the inputs in Figure 21. Relative to a) there appear to be less high frequency and more low frequency elements in c). The diagonal stripe in b) is an artifact.

A-23

- Figure 23 - Photographs showing uniaxial deformation of a rectangular prism of Tennessee marble. Magnification = 3x. (Courtesy of Dr. Syd Peng, U.S.G.M.)
- Figure 24 - Corrected stress/strain curve generated during the deformation experiment pictured in Figure 23. (Courtesy of Dr. Syd Peng, U.S.G.M.) Points 13, 50, 100, 150 and 250 correspond to d, b, c, d, e, respectively in Figures 23 and 25.
- Figure 25 - Maps of the transforms generated by the inputs pictured in Figure 23. c), d), and e) are oval with the major axis approximately horizontal. Rank in order of apparent decrease in spatial frequency: b), d) & e), a), c).

A-24

A-25

A-26

TECHNICAL REPORT SUMMARY

The purposes of this project are (1) to compare and correlate fabrics of suites of genetically related rocks, utilizing optical diffraction analysis and (2) to contribute to the understanding of the mechanics of rock deformation by quantifying fabric changes and relating these to other deformation parameters. Our general methodology rests on the linkage between two types of operation and their respective subject areas, viz. - rock deformation and optical diffraction analysis. During this first year of work, most of our activities were initially in the optical field. During the latter part of the year, increasing emphasis was placed on obtaining rock deformation data, which were then processed optically.

Technical problems which arose earlier in connection with producing adequately dimensioned and shaped rock specimens have largely been eliminated; we can prepare and finish rock slices and produce cylindrical cores of several sizes to required standards. Vibration has caused difficulties in photographing specimens under load; we are bypassing this problem with temporary measures until we have completed the necessary construction and modifications.

Noise in the optical system has been decreased considerably; most of this decrease is due to replacement of the original pin hole in the optical diffraction assembly.

Some minor changes are needed to improve our techniques for mounting inputs for the transform-mapping operation.

A problem remaining in the production of spatial filters concerns the recording of very fine half tones. These should yield to improved photographic techniques on which we are working. We are still working toward improvement of our capability in holographic subtraction and in optical processing of thin sections.

The data on fabrics of rocks undergoing deformation in the laboratory have been recorded on photographic film in a variety of ways and on acetate peels. These data have then been used as inputs in the optical diffraction system.

Outputs from the optical lab have consisted of transforms, maps of transforms and filtered reconstructed images. Examples of these results are given in Figures 16 - 25.

From the results obtained so far, it appears that a decrease in spatial frequencies accompanies loading in tension, and that this can be accounted for by the widening of tension fractures. An increase in spatial frequencies

accompanies loading of uniaxially compressed specimens where the slope of the stress-strain is positive. All of these results point to a preliminary picture that is consistent with experimental rock mechanics.

We have succeeded this past year in standardizing our most frequently used techniques, in establishing a working rock mechanics laboratory, in evaluating capabilities for our needs of a wide range of photographic materials, in producing a wide variety of spatial filters, in developing an effective procedure for mapping transforms, in achieving holographic subtraction of one input from another (paving the way for displaying directly the differences between rock fabrics in a deformation series), in producing transforms with the partially coherent light of a mercury vapor lamp and with a microscope and accessory optics, and in achieving high quality reversal development of photographs.

As the project continues, continuing activity will center on generating and recording more rock deformation data and the processing of these data in the optical diffraction laboratory. Intensities recorded on transform maps will be calibrated and our holographic subtraction capability will be improved.

The mercury vapor-microscope system for optical diffraction analysis will be thoroughly evaluated with refinements made as needed. Work will be extended to biaxial and triaxial deformation experiments.

All of the results achieved so far are entirely consistent with the aims of the project and the program of which it is a constituent. Personnel and facilities are adequate for the tasks ahead. The direction of the work to follow will follow the general direction of the original plans when the project was undertaken.

1. Introduction

1.1 - Purposes and Objectives of the Project

This report covers the first year's work of a three-year study the purposes of which are:

- (a) to develop capabilities of optical diffraction analysis to compare and correlate suites of genetically related rock fabrics, and (b) to contribute to the understanding of the mechanics of rock deformation by quantifying fabric changes and relating these to other deformation parameters.

The special need for quantification of fabric parameters is especially urgent in rock mechanics if the continuing collection of many kinds of data is to be meaningful. The optical analytical techniques being developed will be applicable to other fields, such as resource studies using remote sensing, analysis of contour maps, and the like. Ultimately, this work should contribute to more effective design of structures in rock and of safer and more efficient excavation techniques.

The component objectives of the study are as follows:

- (a) To develop quantitative methods using optical diffraction in order to compare and correlate fabrics of a deformation series so that changes in fabric can be related to deformation curves and other quantitative deformation data.
- (b) To identify and characterize through spatial frequency analysis the critical fracture parameters associated with failure.
- (c) To develop a system of standardized fabric patterns and reference transforms with which fabric inputs can be correlated quantitatively.
- (d) To develop an index of deformation in terms of fabric change, from one input to the next, and to relate this index to deformation history.
- (e) To develop an index of fabric heterogeneity for different directions in a single specimen, to be compared with anisotropy measures based on directional differences in physical behavior in the same specimen.
- (f) To compare fabrics in experimentally deformed rocks with those in several selected equivalent rocks that failed under field conditions.

Increased understanding of the relationships between fabric and mechanical behavior should lead to more accurate prediction of rock behavior in engineering operations and possibly to a better understanding of the reasons for the discrepancies between laboratory and in situ test properties.

1.2 - Background

The feasibility of characterizing two-dimensional displays through their Fourier amplitude transforms has been well established. Likewise, the study of such displays by spatial filtering has also been shown to be practical. Whether the display be photomicrograph or satellite photograph, infra-red or x-ray photograph, contour map or camera lucida drawing, it is practical to depict its spatial frequency makeup by means of Fourier optics.

Beyond the analysis of single displays or inputs are the comparison and analysis of sets of inputs, such as photographs and photomicrographs of suites of like rock specimens that have been deformed under progressively higher loads.

In recent years many data have become available on the mechanical behavior of rocks. It has become eminently clear that for all but very few rocks the classical models of isotropic, homogeneous, ideally elastic bodies are not valid. In the attempt to explain rationally the complex mechanical behavior of rocks, increasing attention has been given to identifying relationships between fabric and mechanical behavior.

Many fabric studies performed to date have yielded results achieved only after very tedious work. Some analytical fabric studies include a subjective element that renders impractical the pooling of results based on work by different operators. We are concerned with developing the means to characterize deformation fabrics more objectively and efficiently.

The experimental techniques required to produce deformation suites of rocks for this study are well established. Standard uniaxial loading and cantilever and third-part loading of rock slices cemented to aluminum beams provide input data. Biaxial and triaxial loading will come in more advanced stages of the work.

The optical diffraction method used in this project is based on work in 1873 by Abbe. With the appearance of the laser in 1960, it became practical to use this method for optical data processing.

The basic technique used is spectral analysis of the input's spatial frequency content by optical diffraction. Figures 1 - 5 summarize the technique. The input is a reduced transparency that functions as a diffraction grating with unknown spatial properties. The source of illumination has precisely known spectral properties, i.e., it radiates coherent monochromatic light. The resulting diffraction pattern is the two-dimensional Fourier amplitude transform of the input image. This transform is a graph of the distribution of orientations and spacings of the elements in the input.

With additional optics the input image can be reconstructed from the light rays that form the diffraction pattern. A filtered, reconstructed image can be formed by blocking out some of the light rays in the plane of the transform. Such filtering can be used to

3

suppress dominant alignments in the input so that obscure features can be detected more easily, and to aid in analyzing complicated distributions by systematically removing different components of the input.

Through their diffraction patterns, orientation fabrics in rocks can be described, regardless of scale, in terms of spacings, directions, elongations, and symmetries.

It is also possible to subtract one input from another to show the net change from one to the other. This is done by a holographic technique, described later in this report, that can be accomplished with slight modifications of the optical system used for the operations described above.

The optical part of this project has required both experimental and theoretical study, plus design and purchase of some optical equipment. Series of fabric inputs from deformation experiments plus series of artificial inputs have provided the main kinds of input data operated on so far.

1.3 - Assumptions and Limitations

A basic assumption underlying the entire project is that there are critical fabric changes related to mechanical behavior and that they are indeed visible within the range of magnifications feasible with the equipment at hand. Related to this assumption is the corollary that the means for recording the fabric changes, viz., conventional photography, photography of specimens treated with fluorescent dye penetrants, and photography of acetate peel replicas of specimen surfaces, will record such fabric changes with sufficient resolution.

Results so far indicate that this assumption and its corollary are reasonable.

A limitation inherent in the optical diffraction method used here is that the inputs are two-dimensional. It is assumed, therefore, that what can be seen on the surfaces of specimens is significant in characterizing and explaining the deformation. This factor has not posed any problems as yet.

Another limitation is that the observation of specimens under load has been restricted to deformation experiments without confining pressure. While this limitation imposes a constraint on generalizing some results, the unconfined loading experiments are indeed an essential step in this work. Fabrics of triaxially loaded specimens will be studied later, although the fabrics will probably be recorded following loading, not during loading.

1.4 - Acknowledgements

We deeply appreciate the cooperation of personnel from the Twin Cities Mining Research Center, U. S. Bureau of Mines, especially for providing input data, i.e., photographs of specimens under load and their deformation curves.

We are also deeply grateful for the logistic and technical support of those personnel from the University of Wisconsin-Milwaukee who have no formal obligation to this project but who have cooperated unselfishly in the critical first year of this undertaking.

2. Methods of Analysis

2.1 - Introduction

The basic optical technique, i.e., optical diffraction analysis, is summarized in Figures 1 - 5 and is explained in papers by the principal investigator and by others, cited in Appendix B. A Conductron LaserScan C120 System constitutes the core of our optical diffraction capability. Data sheets for this work are shown in Appendix C- XII, XIII. The optical diffraction technique is used to analyze changes in rock fabric produced by experimental deformation. High quality photographs and acetate peels are used to record the fabric at successively higher loads or strains. The photographs of specimens and peels are used as inputs for optical analysis.

In this study, both the basic optical operations and the rock deformation experiments (Figures 6 - 13) are routine procedures. Considerable effort and attention have been devoted to optimizing the linkage between the two sets of procedures.

Such optimization requires concern for registration, image quality, and scale factors. Adequate registration and image quality are necessary to achieve consistent, comparable, and sufficiently informative results. The scales at which rock deformation data are recorded depend on both the size features being studied and the dynamic range of the optical analysis system.

Without strong comparability between sets of related inputs, the analysis of fabrics of a deformation series by optical diffraction becomes qualitative, and supporting techniques such as transform mapping and new analytical techniques such as holographic subtraction (Sect. 2.2) become ineffective.

2.2 - Optical Analysis

Photographic Operations

Appendix C-VI contains a summary of film characteristics compiled for optical processing. These characteristics were determined during our quest for high-quality consistent inputs, and clean outputs with low noise levels.

Acetate peels of rock slices undergoing deformation were produced using the standard procedure described in Appendix C-XV, and were then recorded photographically sandwiched between crossed polarizers (Sect. 2.4).

In order to determine the "best" scale to record fabric data, the following techniques were tried:

- 1) 35mm photography using a telemicroscope. The telemicroscope, assembled by Photolastic, Inc., consists of 43mm-86mm Nikkor zoom lens and a Bausch and Lomb microscope with 6X objective and 10X ocular. Appendix C-VIII outlines the procedure for

using this arrangement. The minimum working distance is about 1.2 meters. By focusing on millimeter coordinate paper the following measurements have been recorded:

focal length(mm)	reduction	magnification	field of view(mm)
43	-	-	51
50	20.0	3	45
60	17.5	3.8	39
70	15.0	4.4	32
86	11.0	5.5	26

- 2) Macrophotography using a bellows, 50mm-55mm lens and a 35mm SLR camera. Minolta Technical Bulletin E lists data on working distances (76mm to 36mm), magnifications (1.0 to 3.2) and fields of view (24x36mm to 7.1x11.1mm). If a different focal length lens is used the range of working distances changes but not the possible magnifications nor the possible fields of view, providing the bellows is long enough.
- 3) 35mm photomicrography. Equipment consists of a standard microscope tube with an objective/ocular combination giving 9X magnification. The tube is strapped to a movable track mounted on a tripod.

To date macrophotography, i.e., 2) above, has yielded the most consistent results. Technical problems encountered and future plans on the production of input data are presented in this report in Sections 4 and 6 respectively.

A standard photograph identification code (Appendix C-V) has been established. This allows ready reference between the original rock sample and the final optical output. When used in conjunction with the rock orientation code (Appendix C-IV) and the data logs (Appendix C-I, II, III) an experiment can be replicated quite easily.

Ranges of Inputs

In addition to processing rock fabric data, we have also experimented with optical diffraction analysis of a) closed contours, b) aerial photographs, c) groups of discrete particles of diverse shapes and size distributions, and d) some idealized inputs. Some of the idealized inputs and contour maps have been used for holographic subtraction, covered later in this section. All four types of inputs have been analyzed not only because of their geometric kinship to some rock fabrics, but also because they provide very instructive reference transforms and because they can be used very effectively as test inputs for the analysis and improvement of optical procedures such as spatial filtering.

Filtering

Spatial filtering, which has been discussed in Sec.1.2, is shown schematically in Figure 1 of this report, and was illustrated in Figures 2 and 3 of our semiannual technical report. Filters can be produced in a variety of types (Vanderlugt, 1968). We have utilized both amplitude and complex filters.

The former consist of binary (i.e., opaque) and simulated variable density (variable transmission) filters which operate on the amplitude of the light in the diffraction pattern. The amplitude filters we have on hand are listed in Appendix C-XI. We have produced almost all of our own spatial filters (Sec. 2.4).

Directional band pass and rejection spatial filtering are well-established procedures (Dobrin, Ingalls, and Long, 1965). In order to evaluate possible distortion of directionally filtered images, the spatially filtered image of a given input was placed as an overlay on an unfiltered image of like scale. Also, the negatives of filtered images with differing pass directions were stacked in order to see if the whole image would be reconstructed. This technique showed that some noise was added in the form of "wedge-edge" diffraction, i.e., diffraction by the edges of the filter wedges, but that distortion of the image was negligible.

Frequency filtering can now be accomplished effectively. Although frequency filtering has not been investigated by us as thoroughly as directional filtering, a stacking experiment similar to that mentioned in the previous paragraph, but not as detailed, has been performed with very encouraging results.

In addition, filters have been produced in the form of holographic transforms and holographic reconstructed images (Bromley, et al, 1971). Because these filters are actually records of wavefront information they operate on both the amplitude and phase of the light passing through them. Phase information is related to locations of the diffracting elements within the input plane. This allows us to use these holographic filters for the subtraction of one input that represents the difference between the two inputs. We are well along toward completing development of a capability for efficient holographic subtraction (Appendix C-XVI).

There are many ways of producing holographic transforms and images. To date two of these have been explored by us. These are modified Rayleigh and modified Mach-Zender interferometers. The hardware configurations for producing holograms using these two techniques are illustrated in Figures 14a and 14b. Both systems are described

mathematically and physically by Vanderlugt (1966). Initially we have concentrated on the Rayleigh system because of its simplicity and the availability of hardware. We are now moving toward greater use of the Mach-Zender system.

A Rayleigh-type hologram can be produced by the insertion of a small convex lens in the collimated beam used to illuminate the input. This lens is so placed that a point source of light appears in the input plane next to the input. This point source and the transform lens generate a reference beam incident on the transform plane where the holographic transform can be recorded. The angle between the reference and signal beams is increased (reduced) by increasing (reducing) the lateral distance between the input and the point source. The only additional hardware required for this system is that which holds the auxiliary lens. We have used a Conductron universal centering mount that is a part of our basic complement of optical diffraction equipment.

Disadvantages of the Rayleigh system are: limitation of the size of usable input aperture, introduction of aberrations because the outer portions of the transform lens are utilized, difficulty in regulating the ratio of signal to reference beam intensities, a lack of versatility in arranging the hardware and, for subtraction purposes, only simple inputs can be processed effectively.

The Mach-Zender interferometer uses an off-axis beam. The reference beam can be used in the recording of either holographic transforms or holographic reconstructed images by bringing it "on-axis" to illuminate either a transform plane or an image plane. This type of holographic setup requires two high quality beam splitters, two high quality front surface mirrors and stable mounts and supports for each. We have used two-inch diameter coated pellicle beam splitters by National Photocolor Corp. and front surface mirrors which were on hand; new high quality two-inch diameter mirrors have been ordered and will be used in future holographic work. The beam splitters and mirrors have been mounted in Ealing holders. These in turn have been mounted on rack-and-pinion slide mechanisms manufactured by Edmund Scientific Co. (no. 40,891; 60,572; 60,573). The Edmund slides are attached to base plates manufactured by Conductron so that the assembly can be secured to the bed of the optical bench (Figure 14). This arrangement is quite rigid because it is tied securely to the shock mounted optical bench and will provide great versatility in obtaining clean, efficient optical subtraction of related inputs of considerable complexity.

Optical Processing of Thin Sections

In addition to photographs of rocks undergoing deformation and peels taken therefrom we have also been investigating the use of thin sections of experimentally and naturally deformed rocks.

We originally intended to attempt to process thin sections of rock directly on the LaserScan C120 optical bench and to establish limits within which direct processing would be meaningful. Because some slides generated a transform that was messier than the "smearing" caused by phase variations generated by optical inhomogeneities, test inputs were constructed of only cover glass, slide, or cover glasses mounted to slides using various mounting media. The individual glass elements generated no noise but all combinations did.

In order to determine the geometry of the distortions of the transform, negative transparencies of rectangular coordinate paper were mounted between slides and cover glasses using several mounting media. All of these inputs generated distorted transforms. Among the distorted transforms were some which strongly resembled one-dimensional transforms of a coordinate grid (Dobrin, Ingalls, and Long, 1965). This strongly suggested that astigmatism, chiefly cylindrical, was the major problem; further investigation confirmed this diagnosis.

Thin precision spacers between slide and cover glass would perhaps give a uniform thickness. This procedure was rejected because it would be more time consuming than photographing the thin section and using the resulting negative as an input. Pressing of the section during curing also proved to be an unworkable technique.

For a given degree of surface irregularity, the flatness is a function of the size area being viewed. Thus, by looking at smaller areas of the section the transform should become less distorted. Also, a smaller area should lead to fewer of the phase variations which tend to smear out the transform. This was proved in practice. By masking the input down to a very small area a much less distorted transform was observed.

But two other problems entered here. First the use of coherent light resulted in annoying diffraction effects from the mask and from remaining irregularities in the area of the section being illuminated. Secondly, the area of the section being viewed became so small as to be meaningless.

These problems were overcome by using a mercury vapor lamp as a non-coherent light source and a microscope objective as a transform lens. Any high pressure mercury vapor lamp can be used for illumination in this set-up. To achieve partial coherence, this light is monochromatically filtered and is then passed through a condenser-pinhole arrangement manufactured by Jodon Engineering Associates, Inc., such as LPSF-100 with a 10X objective and a 25 micron diameter pinhole. The beam emerging from the pinhole is then collimated after which it illuminates the input on the microscope stage. Because the location of the transform plane varies with the power of the objective but is always located close to the back of the objective, a telemicroscope is used to view or photograph the transform; a standard microscope ocular is inserted into the microscope tube to view or photograph the area under study.

In order to check the reliability of results using this optical set-up, photographs of the area of the input section generating the transform and the transform itself are obtained. The photograph of the section is then processed on the Conductron set-up using the laser as a light source. The two transforms can then be compared. Results to date have been mutually consistent.

2.3 - Rock Deformation Experiments

Our rock deformation experiments have been performed using established rock mechanics techniques (Figures 6 - 13). Tests so far have been limited to uniaxial deformation of cylinders (Figures 7 - 9) and cantilever and third part loading of 1-2 mm thick rock slices cemented to 10-1/8 x 2 x 1/4" aluminum beams (Figures 10 - 13). Data sheets for these experiments are shown in Appendix C, I - III. Some input data have been provided by the Twin Cities Mining Research Center, U.S.B.M., based on uniaxial experiments by the Center's personnel.

During deformation we have photographed specimens to record changes in the two-dimensional fabric of the rock. Appendix C-V outlines our photograph identification code.

Among the changes we seek to map are microfracture growth, variation in patterns of microfractures, changes in grain shape and/or orientation, development of twinning, changes in reflectance, and so forth.

Experimental results from this work are shown in Figures 16 - 22. In addition, Figures 23 - 25 show the results of work with inputs from uniaxial deformation of a rectangular prism, the inputs having been provided by Dr. S. Peng of U.S.B.M.'s Twin Cities Mining Research Center.

In order to record any fabric changes a variety of photographic equipment has been assembled (Appendix C-IX) and several techniques have been explored (Sect. 2.2).

Because strictly comparable optical inputs are needed (Sect. 2.1) a method of marking the rock samples has been devised. The registration marks for a cylinder were presented in Figure 12 of our semi-annual technical report. For work at a magnified scale we are adopting the convention of affixing a rectangle or square of appropriate size to the specimen in a known and easily determined location (Appendix C-II). In this same vein a template has been devised so that all cantilever-loaded specimens (Figures 10, 11) have identical placement of load and strain gages relative to the rock slice.

The major source of samples so far for our deformation experiments is the U. S. Bureau of Mines "ARPA suite". These are one foot cubes of St. Cloud Gray Granodiorite, Westerly Granite, Barre Granodiorite, Dresser basalt, Sioux Quartzite, Berea Sandstone, Tennessee marble and Salem Limestone.

Samples taken from these cubes are oriented according to the conventions outlined in Appendix C-IV. To simplify the code as much as possible, we have considered mutually perpendicular directions cut normal to the faces of the cubes. The code can readily be expanded for cuts made at other than 90° to the cube faces. However, project personnel will first familiarize themselves with the code in the simple form before the more complex form is presented.

Apparatus for biaxial compression testing has also been set up in the laboratory (Figure 6 e)). Apparatus for triaxial testing is on order. Both biaxial and triaxial tests will be run during the second year of the project.

2.4 - Ancillary Analyses and Developments.

Photography of Acetate Peels

The effectiveness of acetate peels for recording details of rock fabric has been amply demonstrated (Figures 20 - 22). The procedure for preparing the peels is given in Appendix C-XV.

Inputs prepared from the peels are produced by mounting the peels between $2\frac{1}{4}$ " x $2\frac{1}{4}$ " glass plates placed on the 4" x 5" transparency holder of the Bownes Illumitran with a piece of polarizing material directly beneath the "slide." The peels are then photographed at the desired scale with a polarizing filter so that the peel is optically sandwiched between crossed polarizers. This enhances the detail in the peel, and eliminates sources of noise such as saw marks.

Photographic Enlargements and Reduction

We also investigated methods of enlarging, reducing, and changing formats of photographic film. The acquisition of the Bownes

Illumitran allows us to perform these operations. In addition the Illumitran can be used to help correct for under- or over-exposure of film. All these procedures can be carried out with a high degree of uniformity and predictability with a minimum of wasted time and film. Thus, we can preserve the rigid standardization of series of inputs to be compared that is so essential for optical diffraction analysis.

Construction of Standard Spatial Filters

Amplitude spatial filters (Appendix C-XI) were constructed on $8\frac{1}{2}$ x 11" bond paper using black Tempura paint and Letratone patterns (57, 59, 61, 63, 87, 97, 98, 99, 100, 936) and/or a combination of these. These constructions were then photographed using high contrast copy, Plus-x pan, Kodalith, or 10E75 film depending on the filter type. The resulting negatives were contact-printed on Kodak 2" x 2" projector slide plates. These plates can be mounted directly onto the X-Y-Z gate (Sec. 4, #6) for use on the optical bench.

These filters were all designed to cover filtering needs already experienced, or anticipated in the near future. Many filters were constructed in suites, providing incremental variations in filter properties. With the filters on hand it is now possible to perform not only a wide variety of filtering operations, but also to investigate systematically spatial frequency content via a differential approach using incremental series.

Thickness of Rock Slices

Studies are being made to determine the optimum thickness of rock slices for the cantilever and third-part loading experiments. Comparable studies, such as those on optimizing thickness of elastic coatings, are likely to be useful here. However, it is necessary to take into account effects of heterogeneity and anisotropy. It is anticipated that grain size will be one of the constraints, as in the ASTM specification for the diameter of cylindrical specimens.

3. Important Analytical Developments

Mapping of Transforms

Among important developments to date is the ability to map diffraction patterns without going through a photographic process. The hardware necessary and the procedure established are given in Appendix C-X, XIV. Routine production of these transform maps and their calibration in terms of optical power is a very important step toward quantitatively comparing and correlating transforms of related inputs.

Holographic Capability

Development of a holographic capability and the hardware needed have been discussed in Sect. 2.2.

Recording of a hologram for subtraction work is a more involved procedure than the recording of an amplitude transform or reconstructed image. We have used A-G 10E75, 35mm film for recording holograms for monitoring purposes; i.e., to determine signal to reference angle, exposure times, etc. The holograms used for actual subtraction purposes have been recorded on 2" x 3" plates manufactured by GCO, Inc. (HR-123P). These plates have the same emulsion as the 35mm film.

Once the various parameters have been determined for a particular experiment and the hologram recorded, the configuration of the optics used to produce the hologram must remain unchanged to achieve subtraction.

Actual subtraction in our laboratory has so far been confined to geometric inputs using the Rayleigh configuration. The procedure used is summarized in Appendix C-XVI (Brcmley et al, 1971).

The development of holographic capabilities will allow us to subtract one two-dimensional input from another, giving a picture of the visual difference between the two. Thus by subtracting the picture of an undeformed rock from pictures taken while it is undergoing deformation a series of pictures showing only the change in the fabric of the rock as load is increased would be produced.

These "difference pictures" and the calibrated maps of the transforms of the individual inputs should go far in quantitatively comparing the changes in fabric in a deformation series.

Processing Thin Sections

Sect. 2.2 presents a description of our attempts to process thin sections optically. Transforms produced by thin sections have been recorded as has calibration transform corresponding to them. The results are mutually consistent. Ultimately we hope to establish a routine procedure, using common hardware, that will allow us to analyze optically thin sections directly at various magnifications. These data would otherwise be lost or gained only after relatively great expenditures of time and materials.

A possible spinoff from the optical processing of thin sections is the limited optical diffraction analysis of film inputs in any laboratory with a microscope and a high power light source.

Reversal Development

A procedure for reversal development of negative film has also been established (Beward, 1971). Appendix C-VIII contains an outline of the process which is illustrated in Figure 15. The process has yielded excellent results with Plus-x pan film. Its usefulness can be appreciated by anyone who has made positives via the negative-positive route. Not only is time saved but one photographic step is eliminated and thus so is some degradation of quality. Sharper and finer grained transparencies that are of at least as good quality as the negative transparencies have been obtained.

4. Technical Problems Encountered

1 - Sample preparation

Problems encountered in sample preparation can be grouped into two categories: initial and final preparation. The former problem has been solved by fabricating our own rock drill and vise assembly, illustrated in Figure 7 and by contracting with a local quarry to cut 2" x 2" x 12" slabs from the 1 ft. rock cubes (USBM-ARPA suite); these slabs can be handled by our rock saws.

With the recent acquisition of a surface grinder, flatness and squareness gauges, etc., and using other equipment already on hand, the finishing problem has just about been solved. It should be noted that the production of rock slices to date has posed no problems.

We are now organizing our operations to produce specimens to ASTM or equivalent standards on a production basis.

2 - Spurious readings from heated strain gages

The heat generated by photoflood lamps have affected active strain gages during photography of specimens under load. This problem has been overcome by switching to photographic techniques which do not require high temperature illumination.

3 - Vibration during photography of specimens under load

Vibration while photographing rock specimens undergoing deformation has been an annoying problem; the resulting input transparencies are unsuitable for optical diffraction analysis. To date we have bypassed this problem to some degree through patchwork procedures and by taking pictures when ambient vibration levels are low.

A rigid scaffold on which the camera(s) will be supported is under construction. Also, arrangements have been made to stiffen and damp the laboratory benches supporting the deformation equipment.

4 - General photography of specimens under load

Problems in microphotography and macrophotography have arisen in the form of variations in focus, illumination and registration during a given deformation series. The first two problems have been discussed above. The last problem is being solved by appropriate marking of the specimen under examination (Sect. 2.3). Large format high resolution photographs such as those that are now obtainable with a recently acquired Hasselblad 500C will also aid in the solution of all of these problems.

5 - Pinhole adjustment

The condenser-pinhole arrangement on the optical bench was a source of intermittent annoyance and degradation of results during a good portion of the year. Readjustment was very time-consuming. This problem

has been solved by the purchase of a new pinhole assembly that is easily adjustable and in which pinholes are readily replaced. The new set-up also permits use of pinholes of a wide range of sizes, thereby adding to the versatility of the system.

6 - Rotatable input

The problem of rotating the transform about the optic axis to achieve efficient mapping has been solved by rotating the input but this, in turn, led to the problem of mounting the input on a rotatable gate. The present procedure (Appendix C-X) gives satisfactory and very consistent, reproducible results but is somewhat messier and more tedious than we desire for more rapid production of transform maps.

7 - Optical processing of thin sections

Major problems remaining in the optical processing of thin sections are: a low light level from the mercury-vapor source, necessitating very long exposures in order to record the diffraction patterns; coma-type aberrations introduced by slight deviations of elements from center of the optic axis; a rather awkward and time consuming method of alternating transform/input viewing; and a low quality collimating lens.

These problems are being solved, respectively by: our obtaining a more powerful light source which is spectrally enhanced at the wavelength of the monochromatic filter being used (5461A); more precise alignment of optical elements and perhaps tying them all together in a more compact, portable form; use of a centering telescope in the place of the microscope ocular, which will allow viewing of the transform by a simple adjustment of the telescope; and purchase of a high quality collimating lens. Necessary purchases have been initiated. It should be noted that use of the centering telescope will reduce the optical path by $1/4$ to $1/3$, thereby helping mitigate the low light level problem.

Related problems that arose and a discussion of their solutions are presented in Sect. 2.2.

8 - Holographic subtraction

Most of the problems which have arisen and been solved in the undertaking of holographic subtraction are discussed in Sect. 2.2. In addition, a 4" x 5" cut film holder has been modified to hold the hologram for filtering purposes. The center of the holder was cut out and an opening was enclosed with a balsa wood frame to secure the holographic plate to the center of the holder. This arrangement has allowed us to record holograms in a non-dark room and also to use the holograms as subtraction filters.

Related needs remain: preventing emulsion displacements during developing and, more importantly, acquiring suitable space to house our holographic operations. Encouraging starts have been made toward meeting each of these needs.

9 - Production and use of spatial filters

Two problems have arisen in the production and use of spatial filters: i) mounting the filters on the optical bench in a mechanically stable manner, and ii) recording of fine halftone patterns at suitable gray levels.

The first of these problems has been solved by recording the filters on glass as described in Sect. 2.2. The second problem may be solved by using high resolution optics in conjunction with high resolution film and special developing techniques; we are currently the beneficiaries of expert advice on this matter.

5. Results to Date

The results shown in Figures 16 - 25 in this report and in Figure 16 of the semiannual technical report are representative of what we have sought to achieve during the first year of this study.

The results in Figures 16 - 19 are based on work with one of three mutually perpendicular slices for each of which comparable results have been obtained. A second set of three mutually perpendicular slices has been processed identically. Similarly, the results in Figures 20 - 22, using acetate peels, are based on work with one of three mutually perpendicular slices for which comparable results have been obtained. (The slice in Figure 20 is not the same as that in Figure 16.) Again, a second set of three mutually perpendicular slices has been processed identically with the first set, using acetate peels.

Specimens studied in the first of the two categories above, i.e., by direct photography and not with acetate peels, have been photographed in the three different ways described in Sect. 2.2. This multiple approach has been used to evaluate the relative effectiveness of the several techniques for recording fabric.

Although some efforts have been made to highlight growing fractures with fluorescent dye penetrants, we have not yet conducted an evaluation under regular experimental conditions.

About a half-dozen experiments on uniaxial deformation of rock cylinders from the USBM-NASA specimen suite have been conducted, with loading results such as those shown in Figure 9. The type of optical diffraction results obtainable from this operation were presented in Figure 16 of our semiannual technical report.

Most of the specimens we have deformed so far have had linear or nearly linear deformation curves, like those in Figures 9, 13, 17 and 21. (load (lbs.) is plotted in Figures 13, 17, and 21 instead of stress, as in Figure 9, simply as a matter of convenience). One of the strategies in this study is to concentrate recorded observations of specimen fabric in regions of the deformation curve where sudden changes in slope and other prominent nonlinearities occur. In linear or nearly linear cases, the observations are spread out to give broad sampling of the deformation curve.

With regard to the experiment shown in Figures 23 - 25, a set of input photographs, five of which are shown in Figure 23, and the deformation curve (Figure 24) were provided by Dr. Peng of the Twin Cities Mining Research Center, U.S.B.M. Since the curve came into our hands some time after the inputs, we selected for processing the five inputs shown on the basis of their appearance, without benefit of having the stress/strain data. Although the five inputs seem to represent fairly good coverage of the curve, we would have made a somewhat different selection of points had the curve been available when optical processing was started.

Spatial frequency analysis (Figures 18 and 19) of the inputs shown in Figure 16 shows that with increasing load there is a shift in spatial frequency content from higher to lower frequencies. The development with deformation of a fine network of closely spaced fractures would appear as a shift from lower to higher frequencies. In contrast, the widening of fractures and/or the closing of other fractures could generate a frequency shift like the one observed here.

Note the exquisite detail revealed in Figure 20 by the acetate peel method. The slice of Barre granite (Barre Granodiorite) to which the peels were applied here is not the same as that shown in Figure 16, however both slices come from the same one-foot cube and accordingly a comparison of Figures 20 and 16 indicates the greater detail available from the peel method. Again, the spatial frequency shift, as deduced from Figure 22, appears to shift toward lower frequencies. In this case, the comparison between the first and third inputs is that between unloaded specimens, before and after loading.

In the work done with cylinders, as reported and illustrated in our semiannual technical report, there is some tendency for a shift with loading from lower to higher spatial frequencies. It should be noted that the rock slices have been loaded in tension while the cylinders have been loaded in compression, which could account for the contrast in the direction of observed shifts in spatial frequency. The widening of existing cracks in tension and the development of shear and extension cracks in compression would be consistent with these observations, and in fact detailed examination of the inputs suggests some support for such an explanation. However, more detailed work is needed before designating any such conclusions as firm. It will be helpful to examine rock slices in compression as well as in tension; this can be accomplished by loading the aluminum beams with the rock slices on the beams' undersurfaces.

In the deformation series illustrated in Figures 23 - 25, in which a rectangular prism of Tennessee marble was compressed uniaxially, the spatial frequency increases in the region of positive slope of the stress-strain curve; this is consistent with our observations so far for cylinders. The frequency quickly drops where the curve starts to turn downward and then increases slightly on the negative slope. The spatial frequencies are higher in the final input than they are in the unloaded input. The transforms of the inputs on the negative slope are oval with horizontal long axes. All of this suggests that we are mapping the onset with failure of vertical extension fractures and some additional fracturing as deformation continues.

The foregoing are only tentative interpretations, but the results so far for slices, cylinders, and the prism all seem to be mutually consistent. With the acquisition of additional data, continuing refinement of technique, and further study of details, we fully expect to come up with some useful, firm conclusions. It will help greatly to obtain quantitative data that will measure the total frequency content in different frequency bands, so that we can plot stress or strain versus incremental spatial frequency; we have available the basic electro-optical hardware to develop this capability.

Beyond the technical results described above, we have accomplished the following during the past year:

We have standardized and made routine many operations in the optical and rock mechanics laboratories.

We have established a working rock mechanics laboratory, with the capability of deforming rocks uniaxially, biaxially and flexurally.

We can now prepare our own rock slices, can produce cylindrical specimen of several diameters and have acquired the equipment necessary for finishing cylinders according to ASTM and USBM standards.

We have determined the characteristics of photographic film used in optical analysis and have established techniques for recording data at various scales and formats while retaining comparability of results.

We have produced a collection of reference transforms and a variety of specialized spatial filters. The filters have been mounted on glass plates and have been used in an X-Y-O gate assembled by us for this purpose.

A method of mapping transforms has been developed in which the input transparency is rotated about the optic axis to yield a spoke assembly of intensity profiles. We are currently working with a laser power meter to develop a practical method for calibrating intensities recorded in these maps.

Holographic transforms and holographic reconstructed images have been produced. We have used both modified Rayleigh and modified Mach-Zender type interferometers. The holographic transforms have been used successfully for optical subtraction of simple paired inputs of a dot pattern (removing particular dots), a simulated dendritic pattern (showing net growth of the branching network), and a simulated rock fabric pattern (showing development of twinning).

We have successfully produced transforms using partially coherent mercury vapor light as a source and a standard microscope plus auxiliary optics as the optical system. This approach appears to provide some possibilities for the convenient use of optical diffraction analysis in a variety of applications, especially those with thin sections as inputs. Consistent transforms generated by thin sections have been recorded.

High quality results have been achieved with reversal development of negative film. This will permit considerable saving in time over the negative-positive procedure and does not require special positive film. The quality of results achieved is quite good enough for preparing inputs for optical diffraction analysis. In fact, the results are distinctly superior in sharpness to many of those obtained earlier through contact printing of 35mm transparencies.

6. Implications for Further Research

The technical results achieved so far indicate that we are on the right track and that the general direction of the research will follow original plans. Therefore, we will concentrate on recording more deformation data at appropriate scales; this will include use of results from the acetate peel and fluorescent dye penetrant methods. Additional data and experience are needed to determine the optimum range of scales at which to record the fabrics of specimens under load; present indications are that for the types of rocks worked with so far, magnifications of 10X to 100X will yield the most useful fabric data.

Research efforts in the optical laboratory will concentrate on the calibration of transform maps, the achievement of routine holographic subtraction of related inputs, development of the mercury vapor system for the analysis of thin sections, expansion of our amplitude and complex filtering capabilities and the continued upgrading of our photographic techniques.

We will also begin to obtain data on changes in fabrics of triaxially deformed specimens. This will be done by carrying cylindrical specimens to specified axial and radial loads and photographing medial sections cut along their axes. One specimen will have to be sacrificed for each data point, and the photographs will be made following unloading. That this technique will yield useful results is clearly indicated by the results of our earlier study (Pincus, 1969a, Part III) and by the present study.

7. Special Comments

Other related research projects in which we are involved are providing test materials and knowhow of benefit to the conduct of this project, and vice versa. Those projects include a study of the effects of rock alteration, joint fillings, and fracture geometry on mechanical behavior of rocks, especially from block-caving operations. We are also measuring triaxial-acoustic properties of rocks from block-caving areas. Fabric analysis is an important aspect of these studies.

As indicated in our semiannual technical report, we are also studying the transforms of separated particles of different shapes and sizes to determine empirically the effects of different configurations, shapes, spacings, and sample size. As the particles are "moved" toward each other until they come in contact, they achieve the spatial configuration of the fabrics of some rocks.

All of these projects, which are under the direction of the Principal Investigator, hang together very nicely, the whole of the capabilities available exceeding the sum of the individual projects' capabilities.

8. Concluding Remarks

The technical skill of the projects' personnel and the major items of equipment on hand, on order, or otherwise available for use are appropriate for the needs of this study.

The basic research design appears to be sound. The results achieved so far have been quite encouraging.

Work during the coming months will be essentially like that during the past few months. Considerable emphasis will be placed on continuing acquisition of fabric data, further refinement of techniques, and increasing application of newly acquired capabilities such as holographic subtraction.

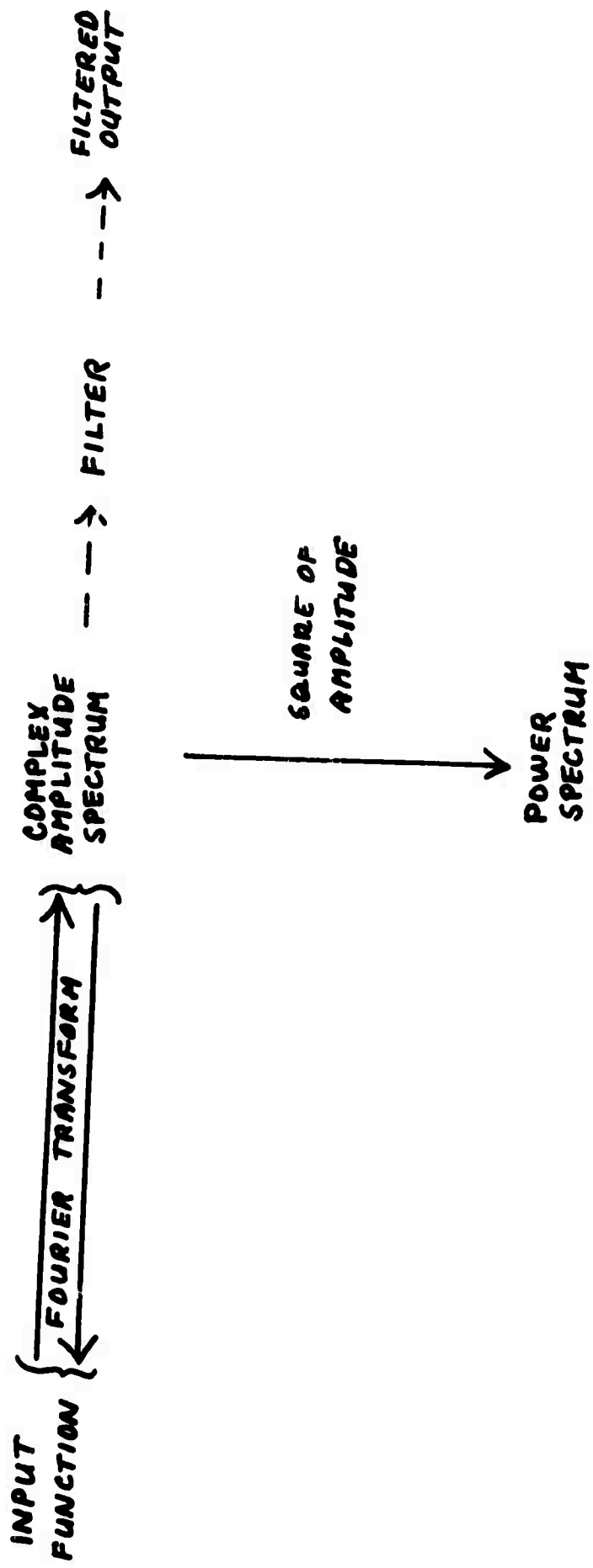


Figure 1. Schematic diagram for optical diffraction analysis. The two products are the transform (spectrum) and the filtered output.

PRODUCTION OF FRINGES IN YOUNG'S DOUBLE SLIT EXPERIMENT

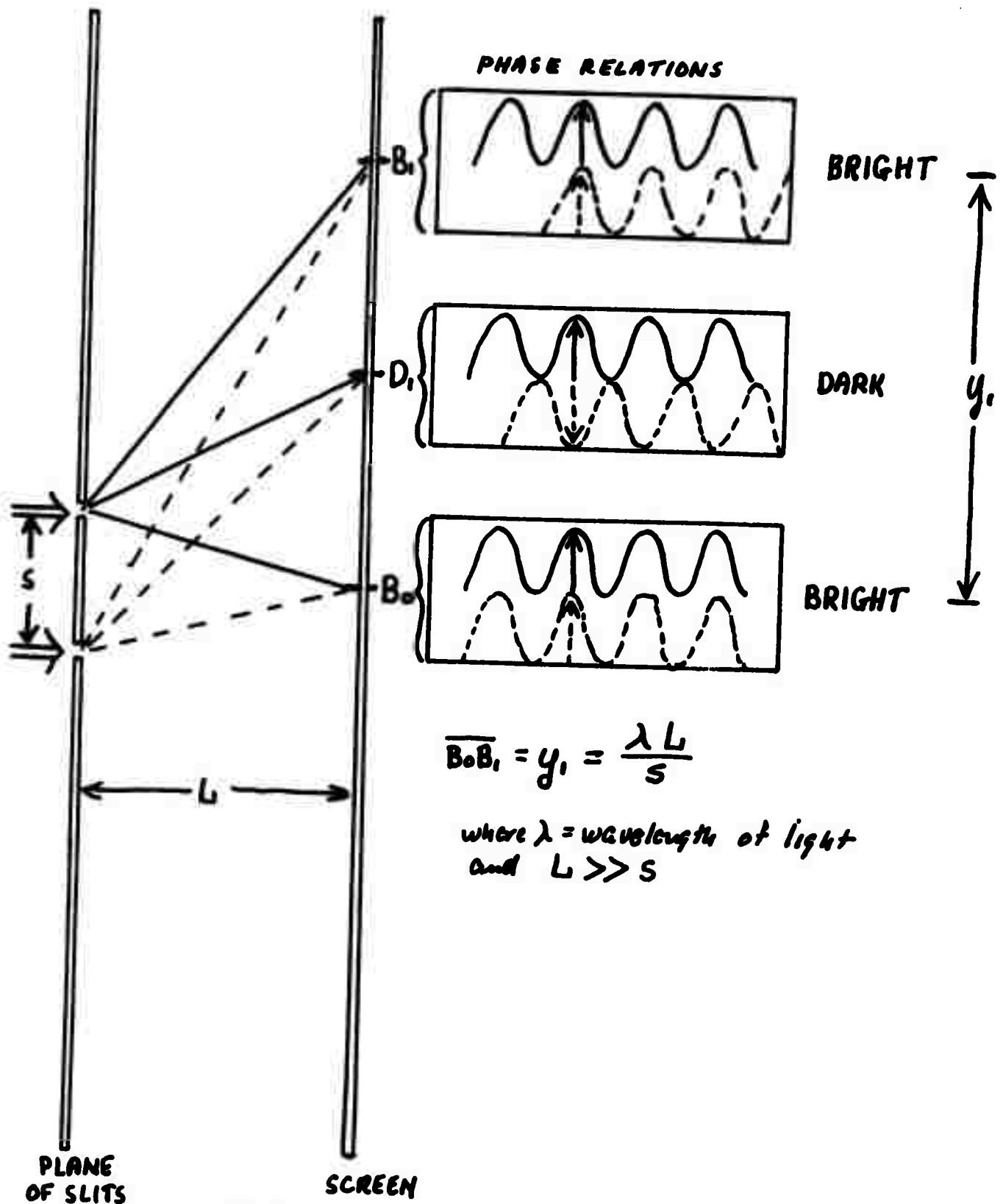
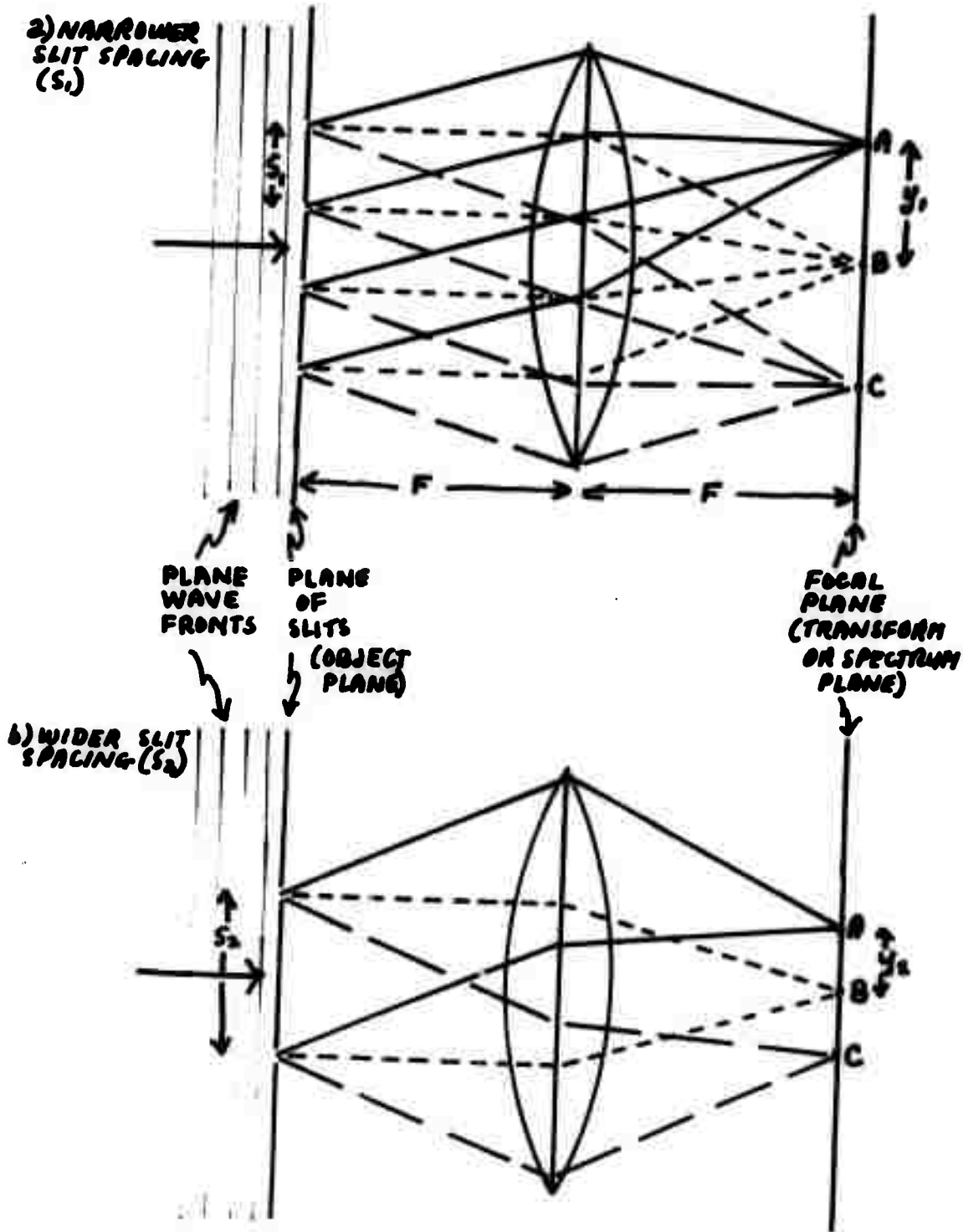


Figure 2. Young's double-slit experiment. $B_1 B_0$ (or y_1) varies with spatial frequency ($1/s$) in the input plane.

After Atkins, 1965, Fig. 2-11.

SPATIAL FREQUENCY ANALYSIS BY DIFFRACTION



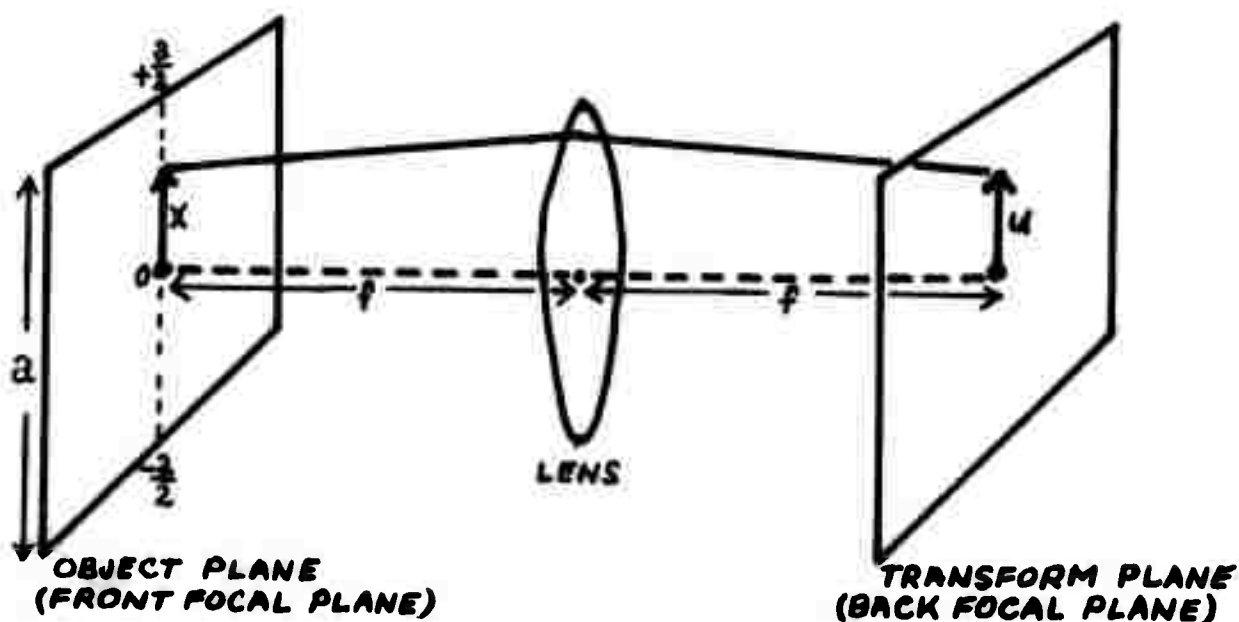
- - - - ZERO ORDER
 / / / FIRST ORDER (UP)
 \ \ \ FIRST ORDER (DOWN)

{ A - FIRST ORDER POINT (UP)
 { B - ZERO ORDER POINT
 { C - FIRST ORDER POINT (DOWN)

$\begin{cases} s_1 = s_2/2 \\ y_1 = 2y_2 \end{cases}$

Figure 3. Fraunhofer diffraction with a lens. y in the transform plane varies with $1/s$ in the input plane.

AFTER SHULMAN, 1966, Fig. 17 and other illustrations.



$f(x)$ input (transmission) function as a function of the position coordinate x in the object plane

$F(u)$ complex amplitude as a function of the position coordinate u in the transform plane

f focal length of lens

λ wavelength of incident light

$$\text{Then, } F(u) = \int_{-\frac{a}{2}}^{+\frac{a}{2}} f(x) e^{-i2\pi xu/\lambda f} dx$$

gives the complex amplitude in the transform plane. The variable sensed is the intensity, or amplitude squared. The complex exponent expresses the phase difference along the optical path. The variation in amplitude along the u coordinate depends on this variation in phase and on the input function $f(x)$.

If y and v are the horizontal coordinates in the object and transform planes, respectively, then the two-dimensional Fourier transform is given by

$$F(u,v) = \iint f(x,y) e^{-i2\pi(ux+vy)/\lambda f} dx dy$$

Figure 4. Fourier transform relationships in a single lens system.

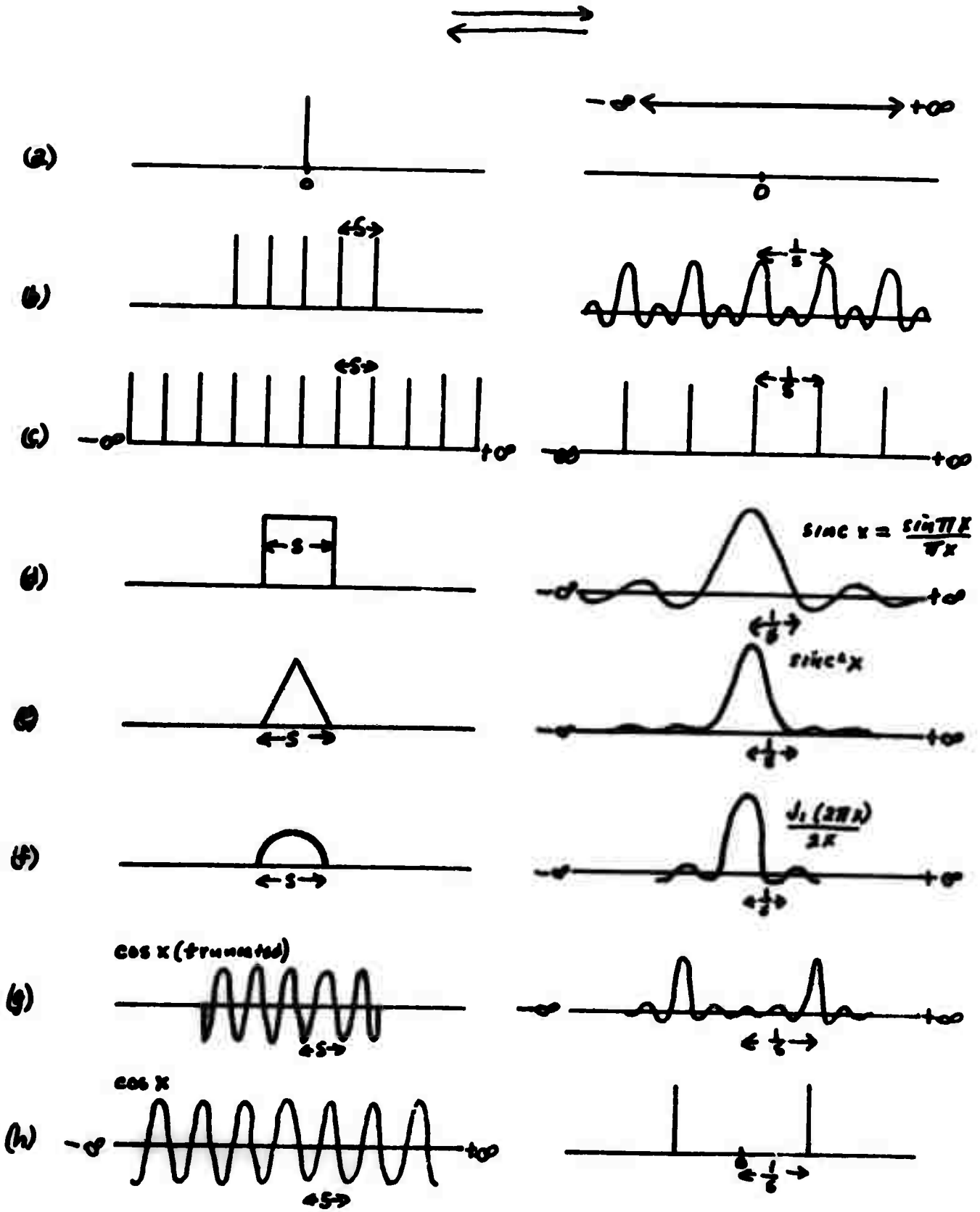


Figure 5. Some Fourier transform pairs, (a)-(h).

After Peterson and Dobrin, 1966 and Bracewell, 1965

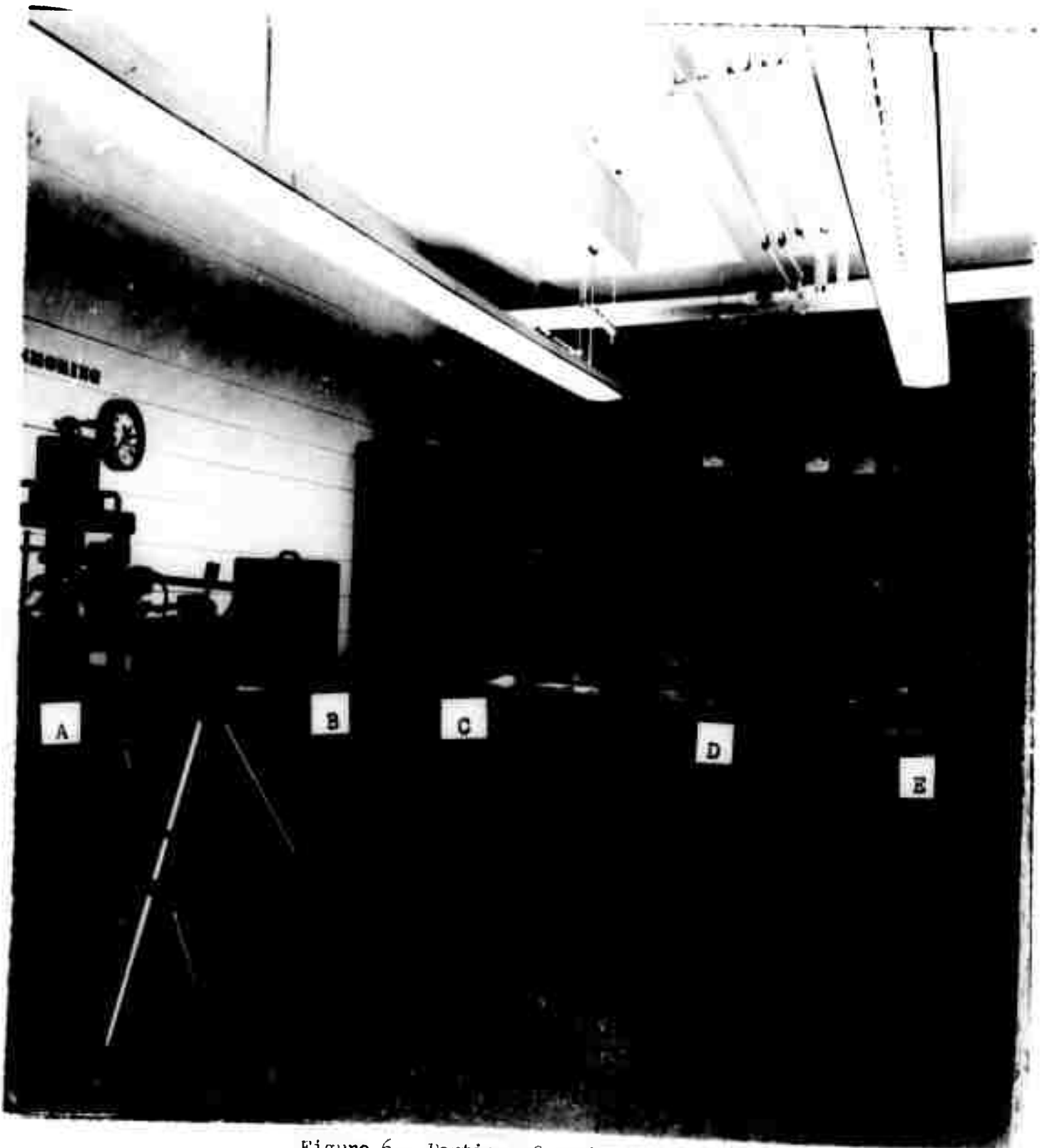


Figure 6 - Portion of rock mechanics laboratory. From left to right: a) uniaxial set-up (details in Figure 8); b) electrical hardware for strain gage work (details in Figure 12); c) rock slice set-up (details in Figure 10); d) third-part loading set-up; e) biaxial set-up.

NOT REPRODUCIBLE

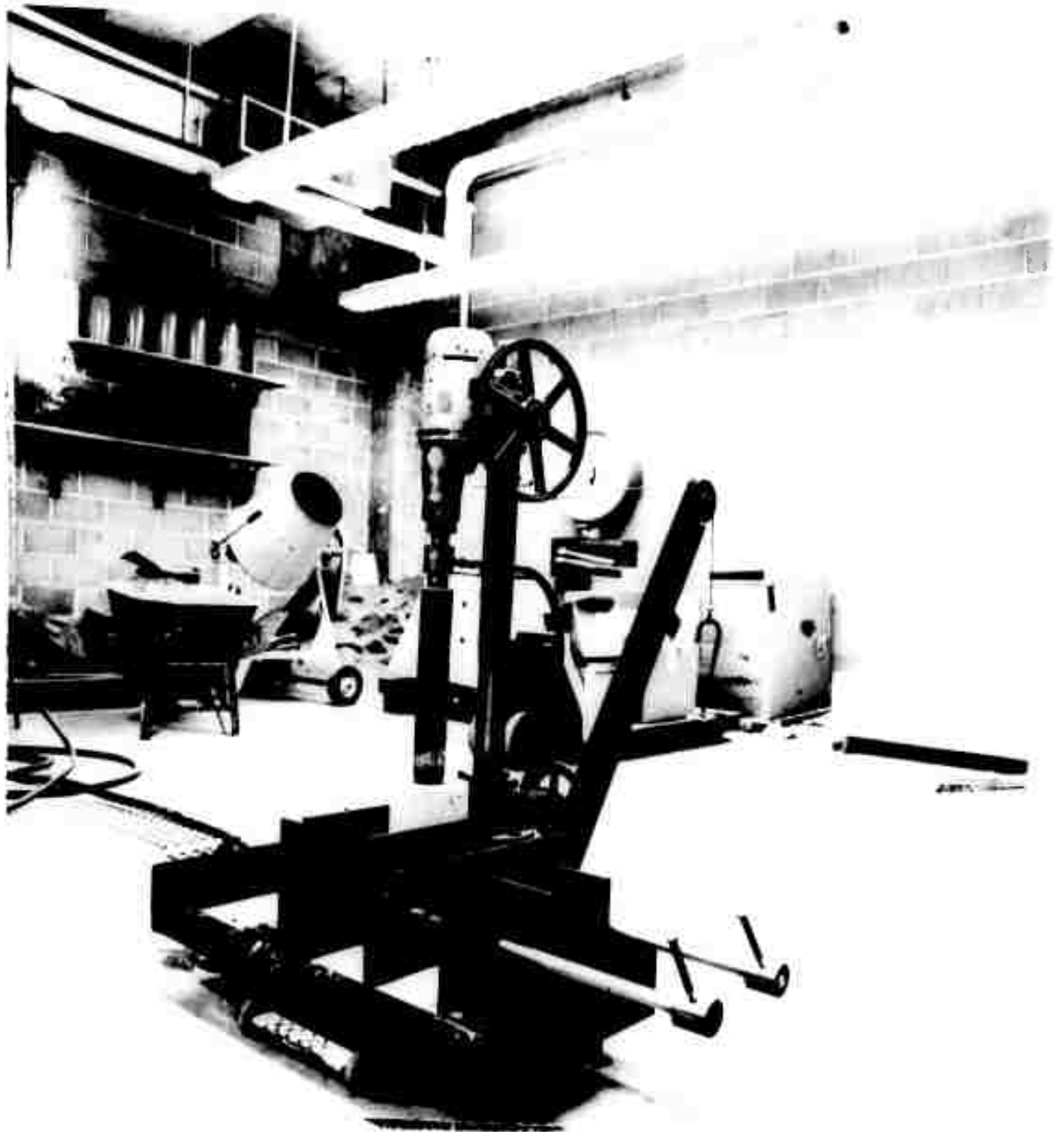


Figure 7 - Rock drill used for preparing cylindrical specimens. NX thin-walled bit shown cutting core from large concrete test cylinder. Base clamp is designed to hold irregular specimens.

NOT REPRODUCIBLE

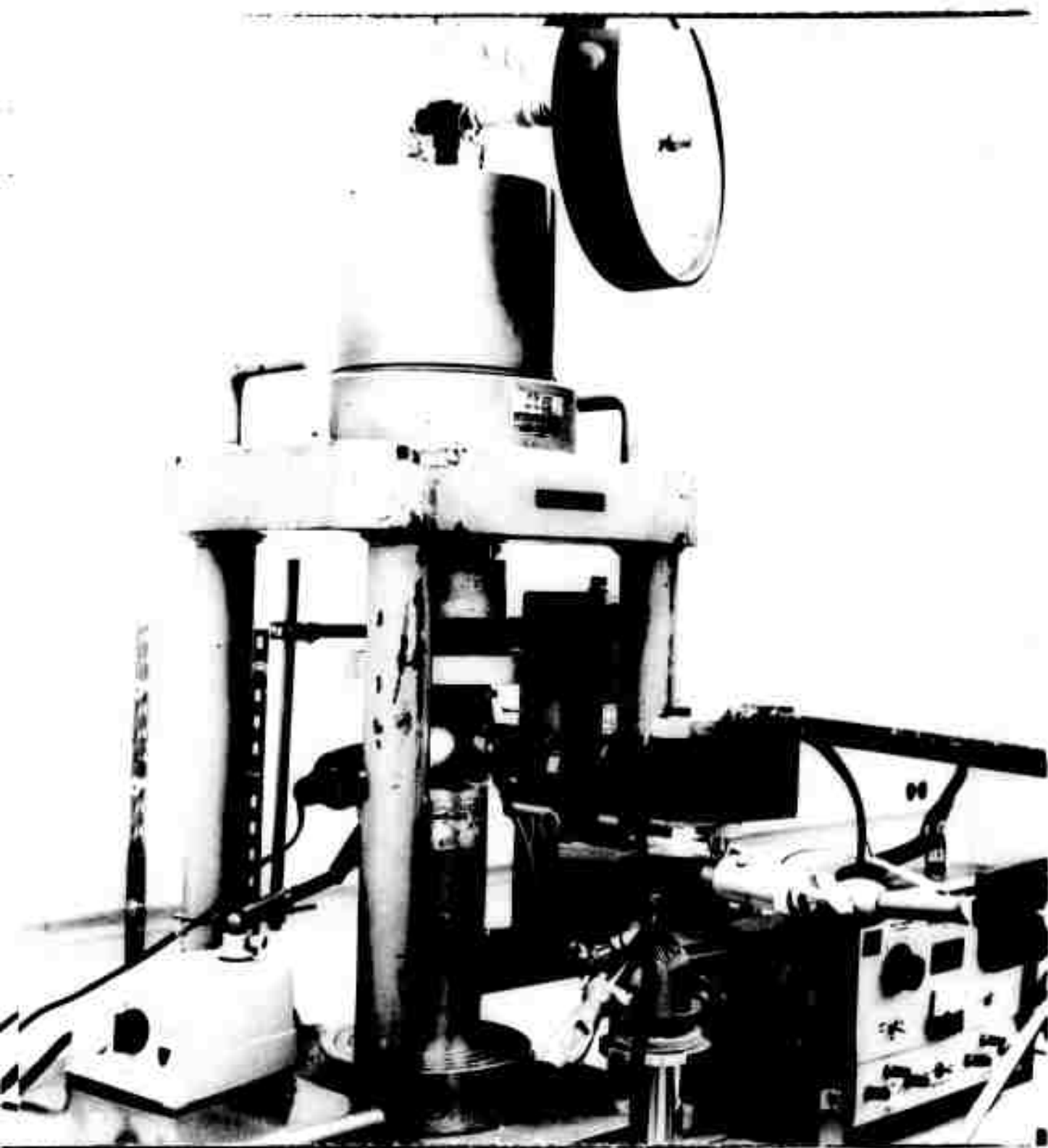


Figure 8 - Uniaxial set-up with photographic equipment for recording surface fabric during loading.

NOT REPRODUCIBLE

Typical Results of
Uniaxial Compression Test
Stress - Strain Curve

A-9

Test Identification No. _____

Rock Type: Charcoal Granite

E: 11.0×10^6 psi

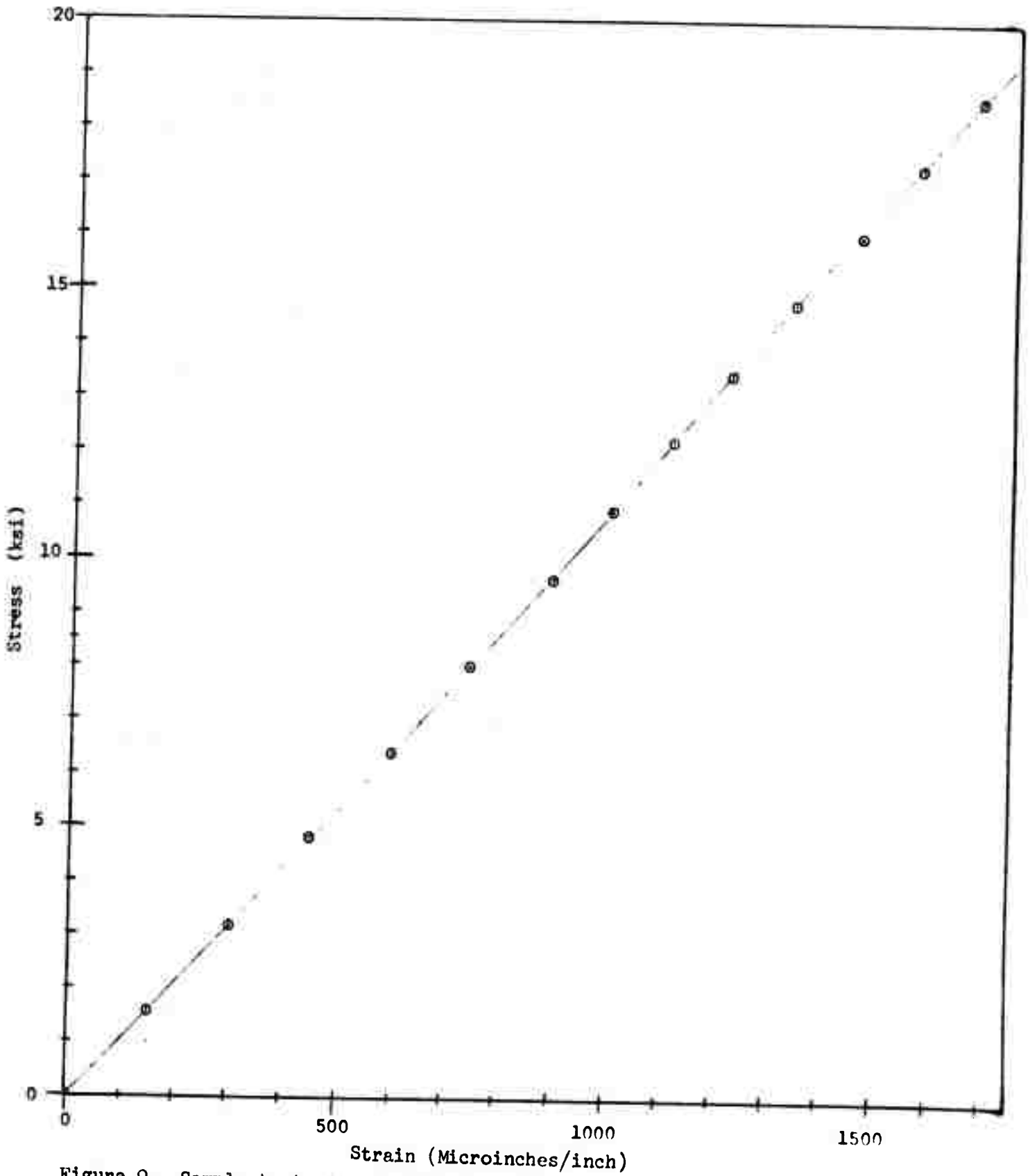


Figure 9 - Sample test results from uniaxial loading as shown in Figure 8.

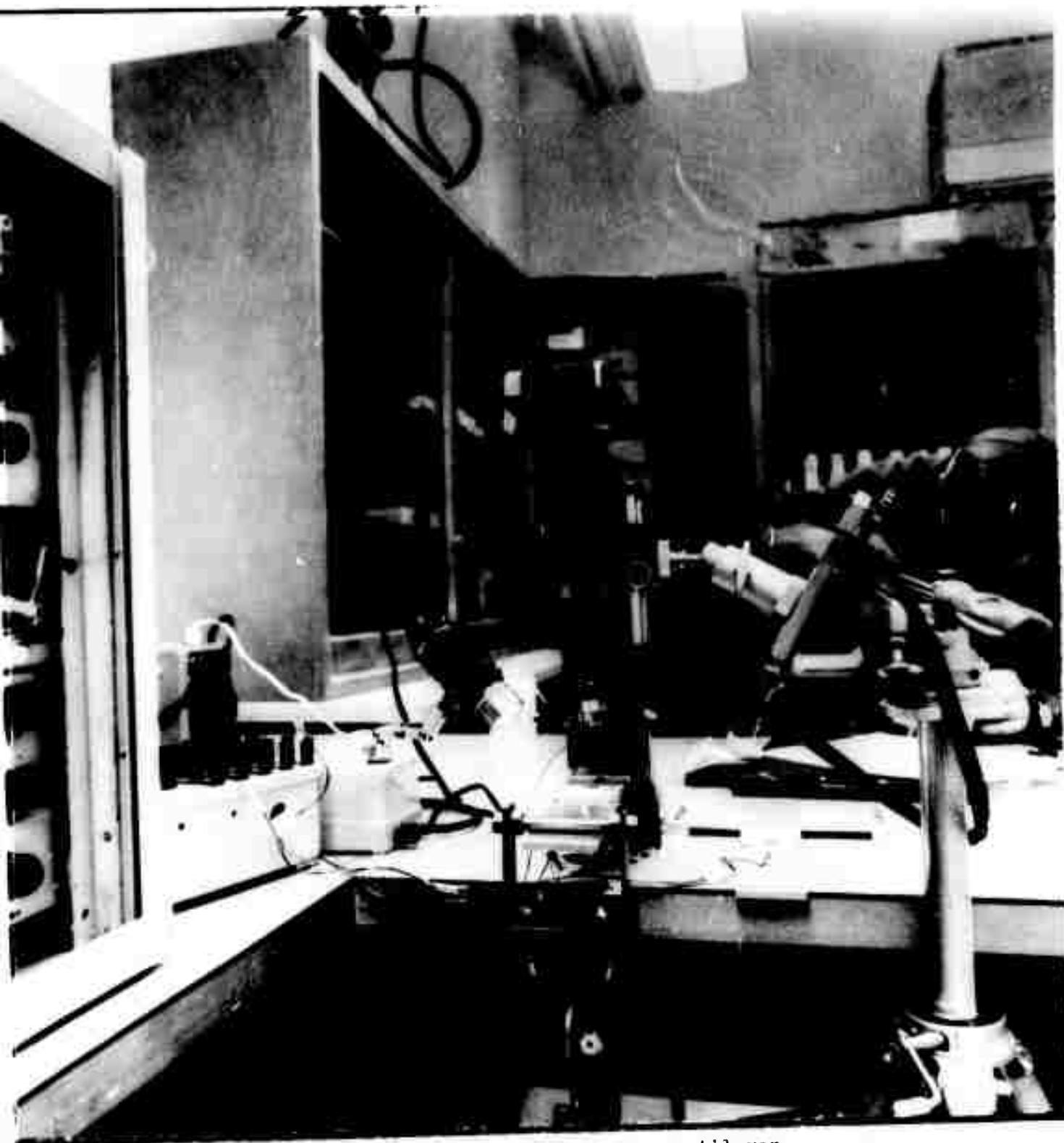


Figure 10 - Rock slice set-up, cantilever loading. Rock slice is cemented to loaded aluminum beam. Slice and beam to right support dummy gage for temperature compensation. Photographic equipment above slice records surface fabric during loading.

NOT REPRODUCIBLE

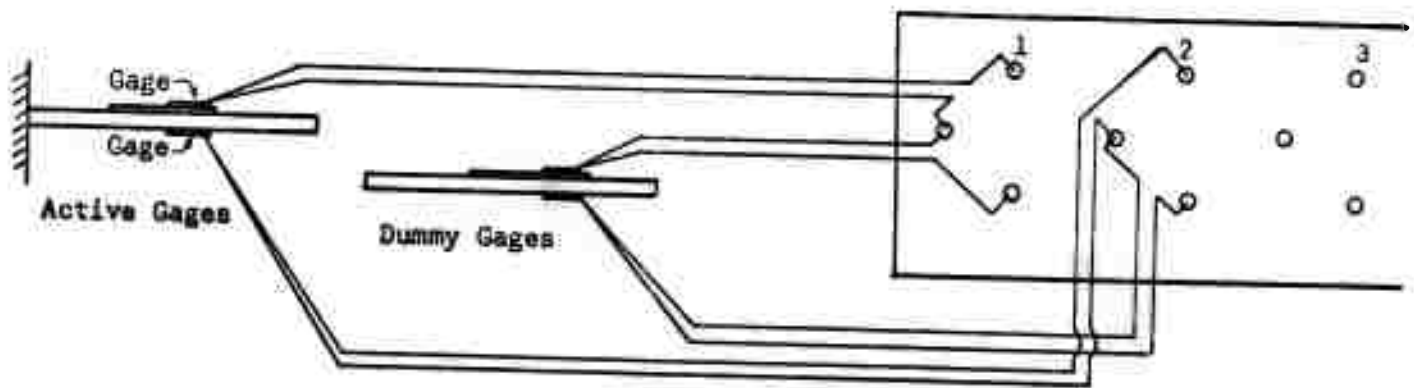


Figure 11. Strain gage circuitry for rock slice test using the cantilever loading assembly

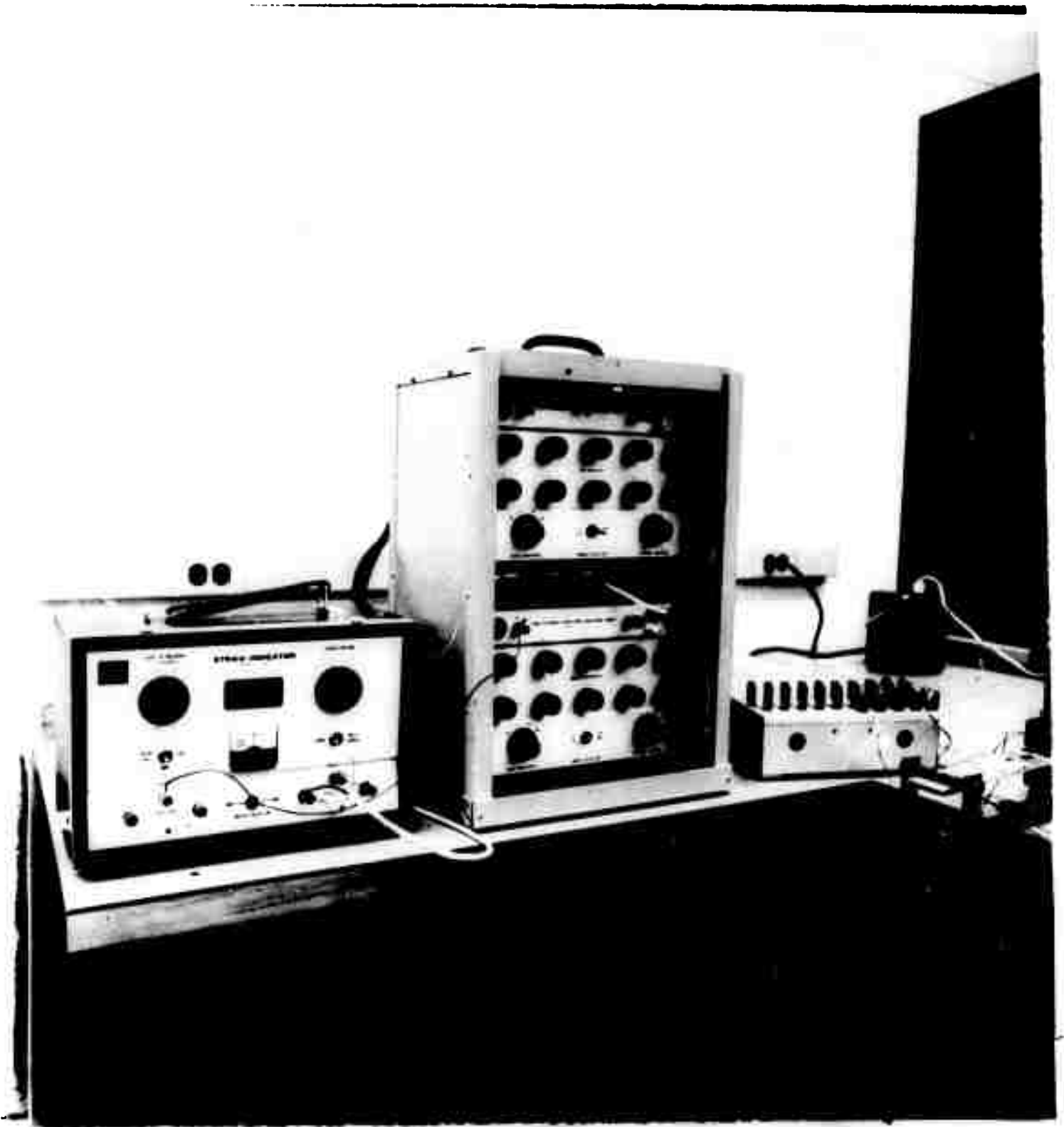


Figure 12 - Electrical hardware for strain gage work. From left to right: indicator unit, stacked switching and balancing units, quick-connect junction box.

NOT REPRODUCIBLE

Figure 13 - Sample test results from cantilever loading as shown in Figure 10, using instrumentation of Figures 11 and 12.

Typical Results of
Rock Slice Test Load - Strain Curve

A-13

Test Identification No. _____
Rock Type: Barre Granite

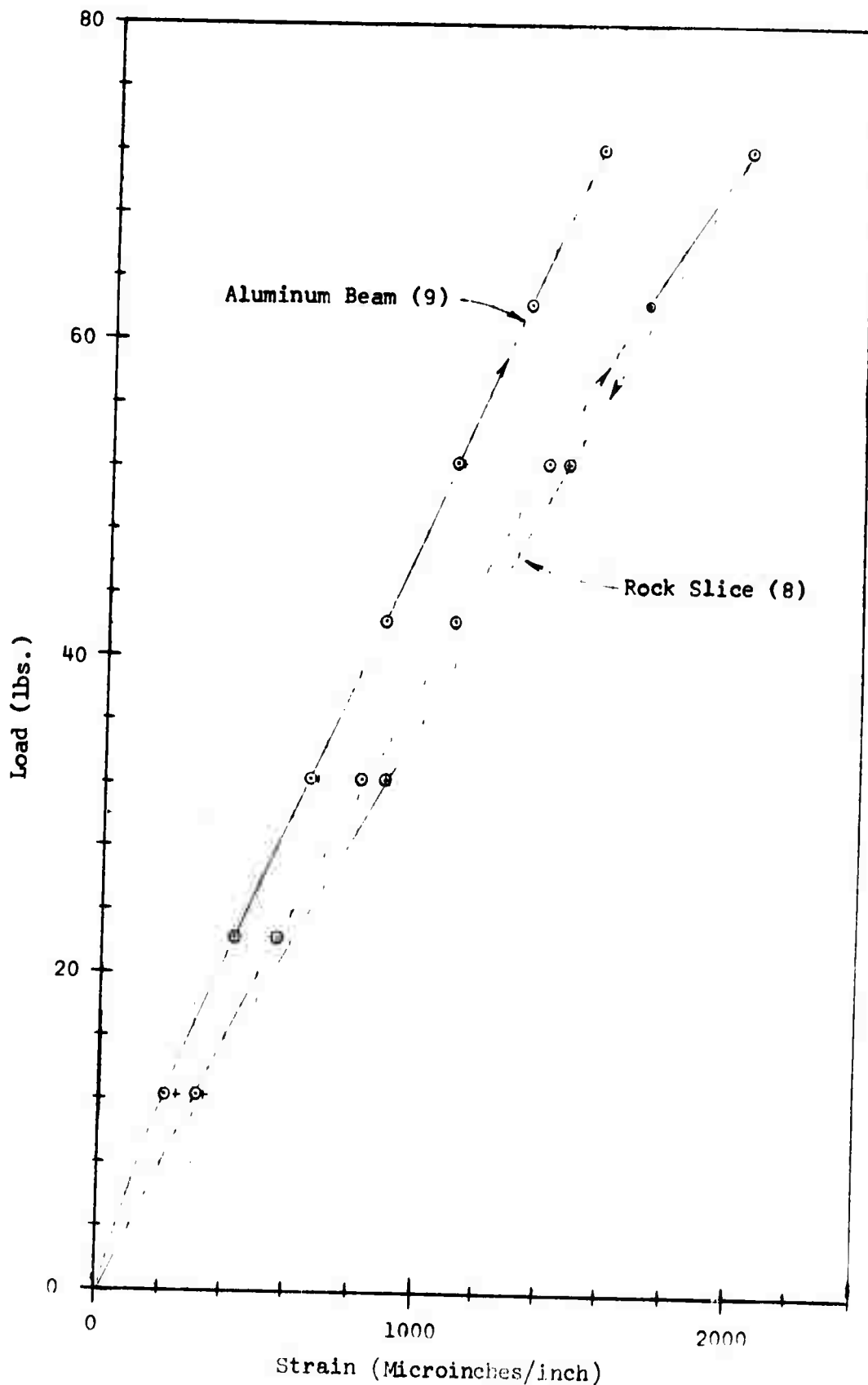
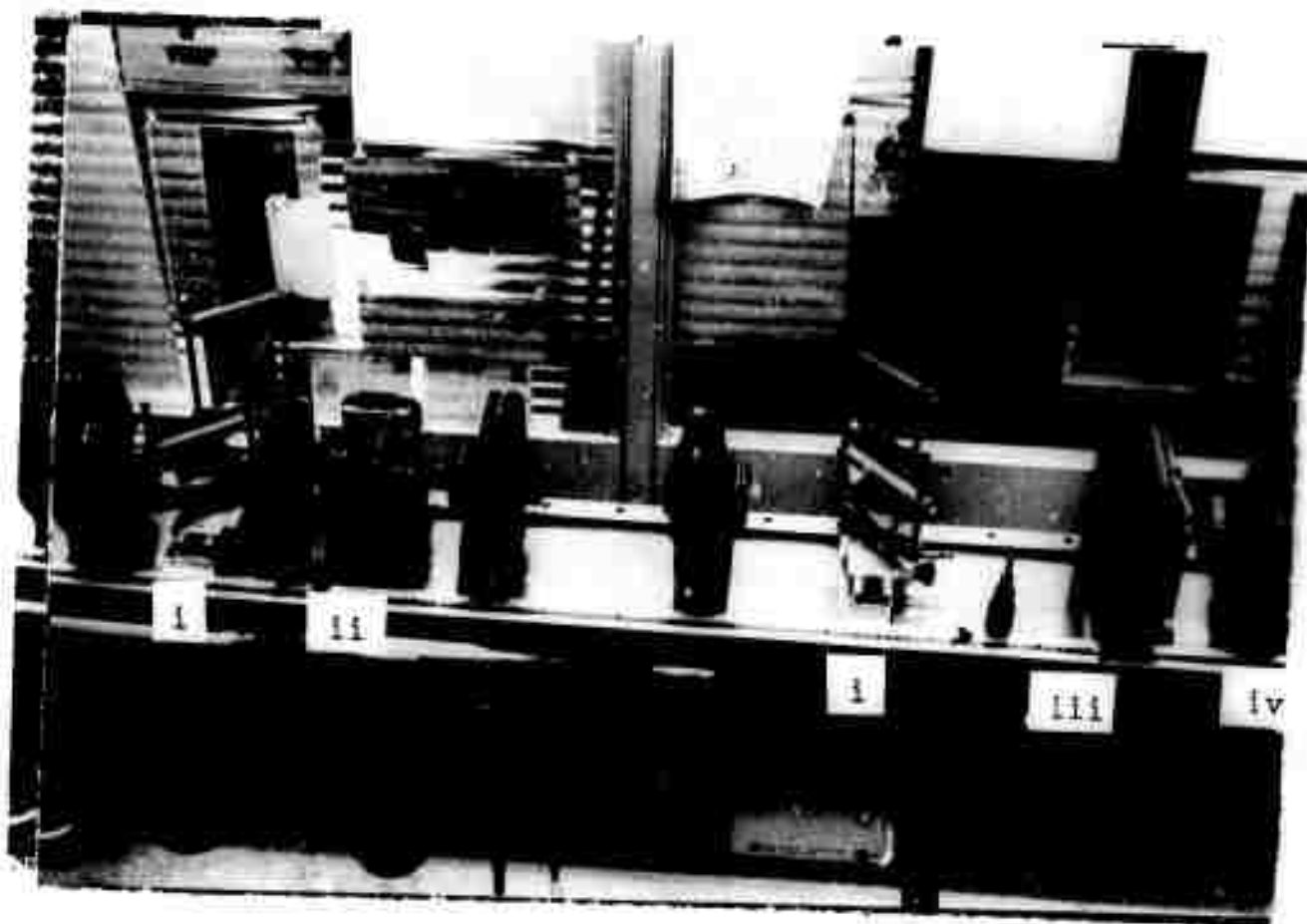




Figure 14 - Configurations of components on the optical bench for producing holographic transforms.

a) Rayleigh configuration. A small lens at position *i* generates a point source of light in the input plane *ii*. The holographic transform is recorded at *iii*.

NOT REPRODUCIBLE



b) Mach-Zender configuration. Beam splitters are at i, the input at ii, and the holographic transform is recorded at iii. This configuration will produce holographic reconstructed images if the second beam splitter-mirror assembly is positioned beyond the reconstruction objectives iv.

NOT REPRODUCIBLE

PHOTO SCIENTIST, March 1971

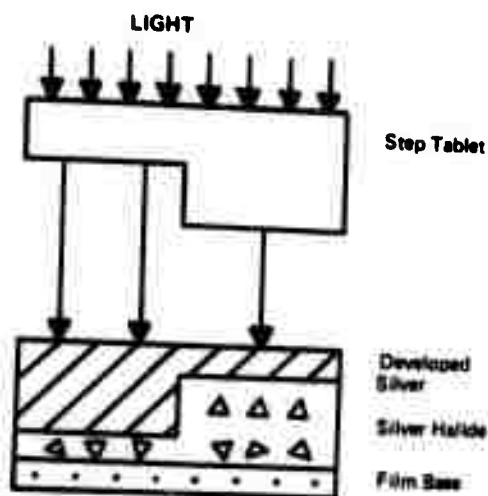


Figure 1. Exposure and First Development

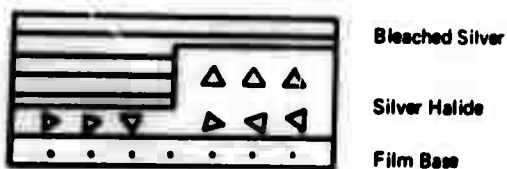


Figure 2. After Bleaching

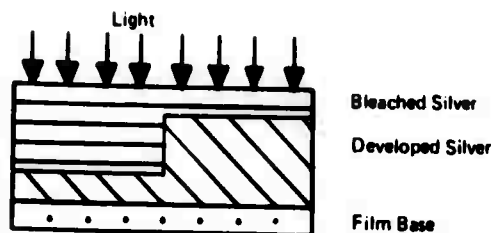


Figure 3. Re-exposure and Second Development

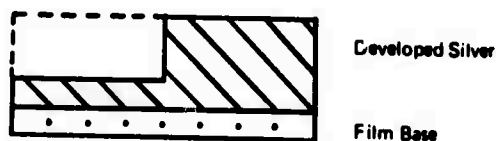


Figure 4. Fixed Film with Positive Image

The theory of processing is shown in the following figures. In figure 1, light is modulated, as upon passing through a step tablet, and strikes the film. On development, the appropriate amount of silver is reduced in the film. In figure 2, the film is bleached to convert the metallic silver into a silver salt not sensitive to light. The excess bleach solution is neutralized with a clearing bath, and the film is exposed to a uniform light. This exposure renders the silver halide still in the film developable in the second developer, as shown in figure 3. In figure 4, the silver salts still in the emulsion are removed by solubilization in the fixer solution, and the silver remaining duplicates the densities of the object.

—Illustrations by David J. Binko

Figure 15 - A diagrammatic representation of the reversal development process. From Beward, 1971.

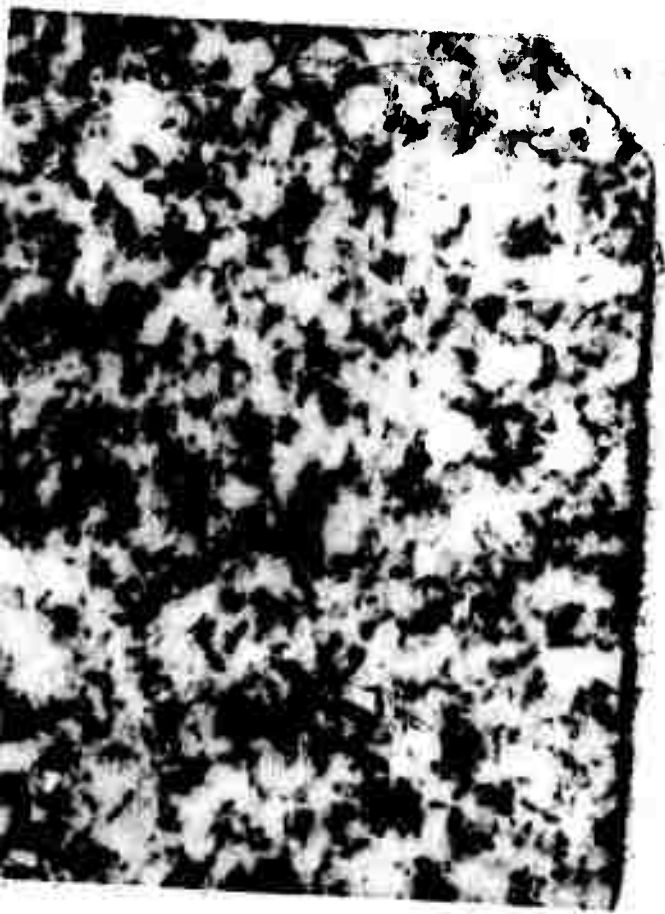
NOT REPRODUCIBLE



a



b



c

NOT REPRODUCIBLE

Figure 10 - Photographs of a slice of barre granite (face 7) undergoing cantilever deformation. Magnification = 2.5x. Load on the cantilever is to the right. The pictures a, b, c correspond to the points A1, A5, A9 on the curve in Figure 17.

Test ID No. C003 A-2

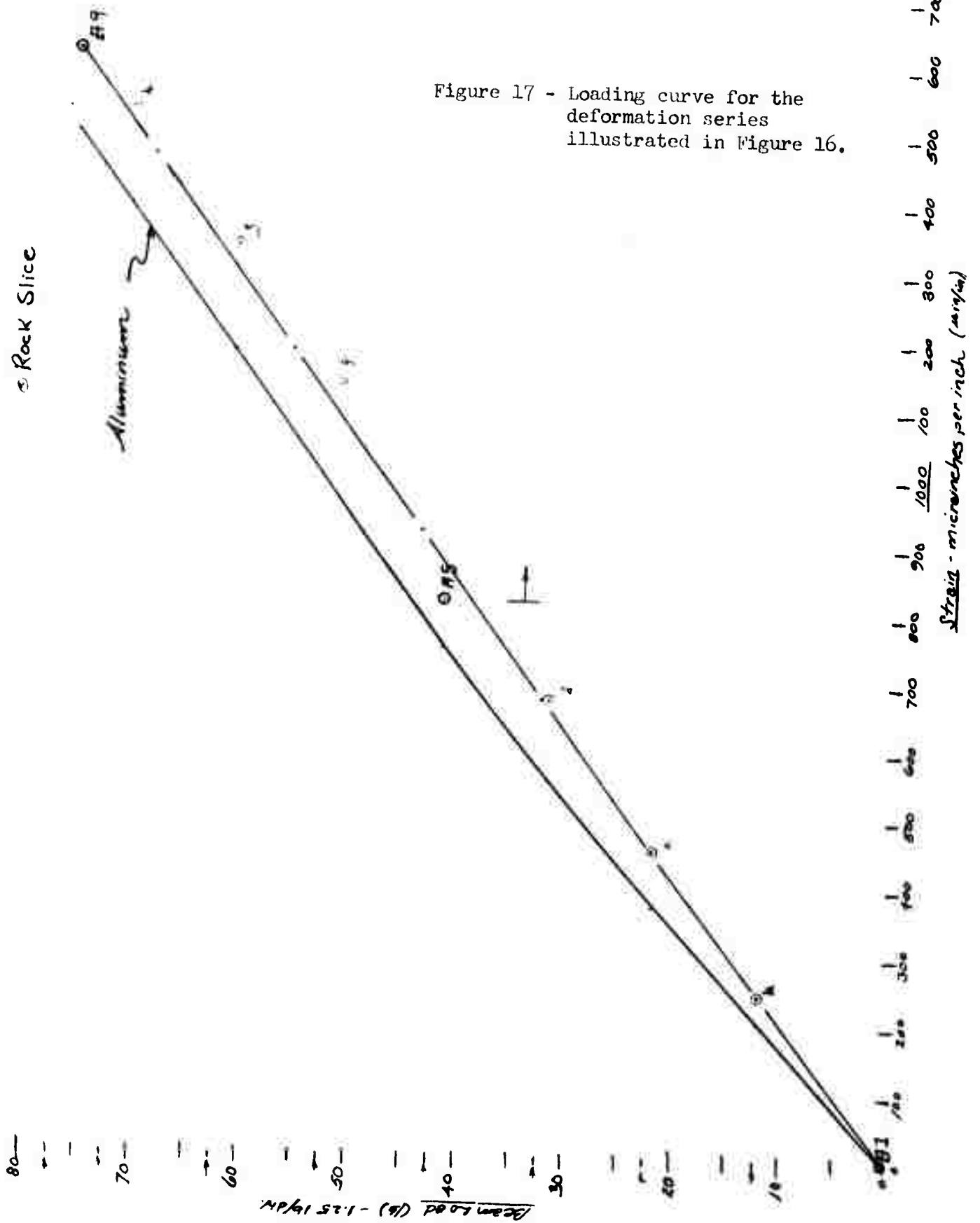
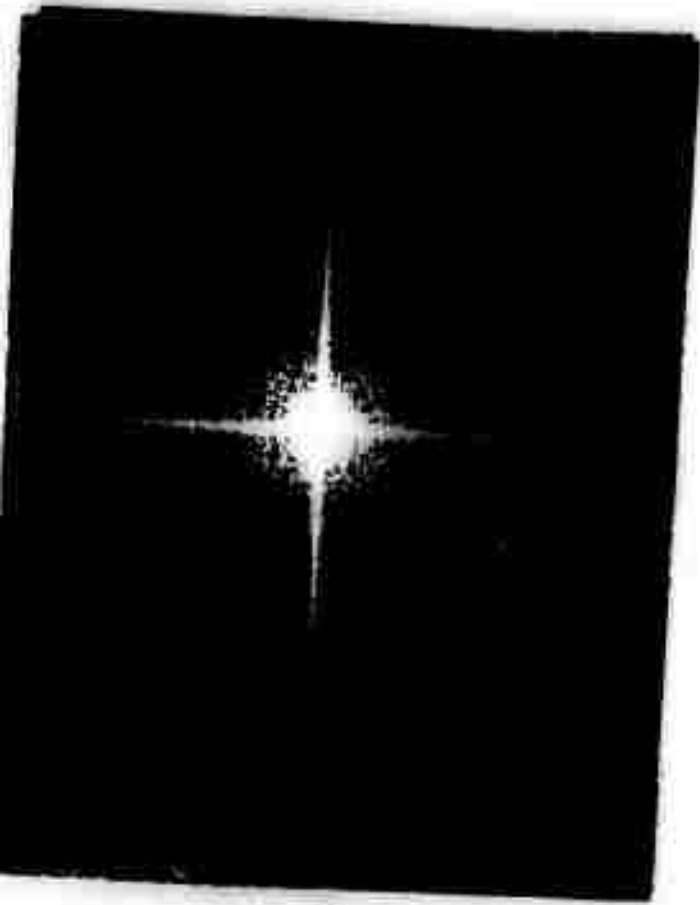
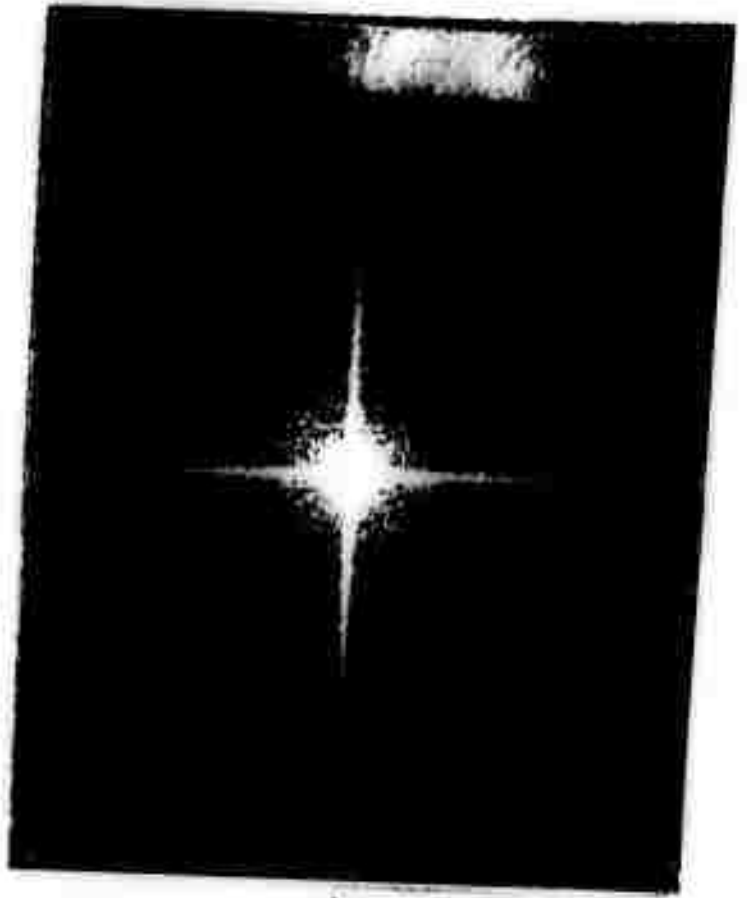


Figure 17 - Loading curve for the deformation series illustrated in Figure 16.



a



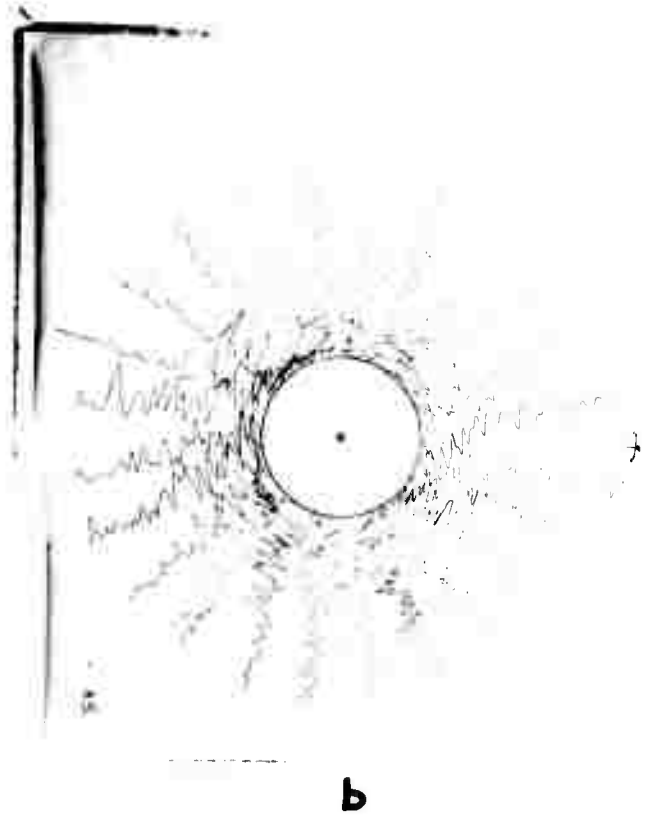
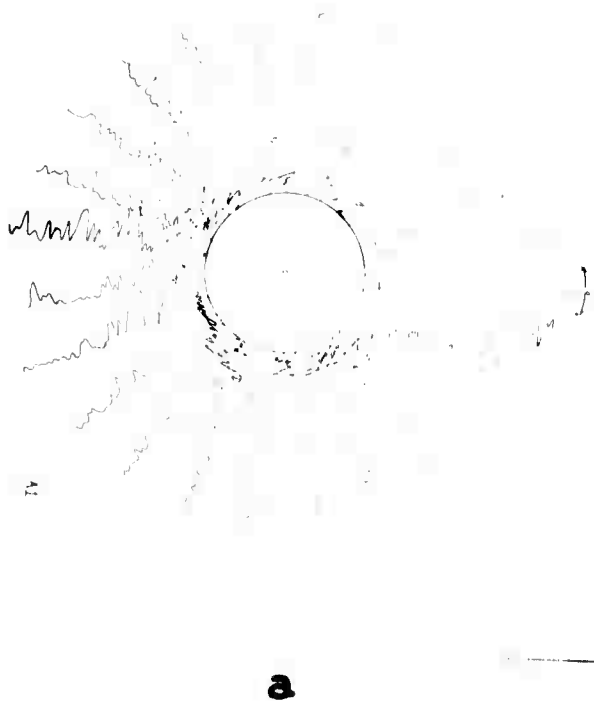
b



c

NOT REPRODUCIBLE

Figure 18 - Transforms of inputs in Figure 17. b) and c) are almost identical and show less high frequency content than a).



NOT REPRODUCIBLE

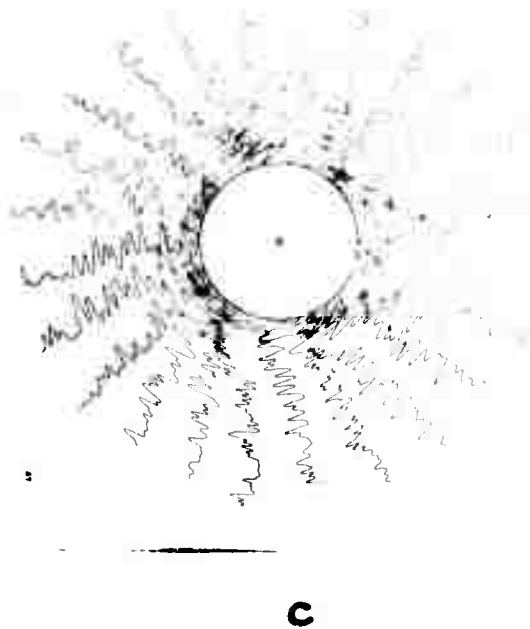


Figure 19 - Maps of the transforms illustrated in Figure 18. There is more low frequency content in b) and c) than in a). c) appears to be more uniform than b) in the directional distribution of diffraction elements.



a



b

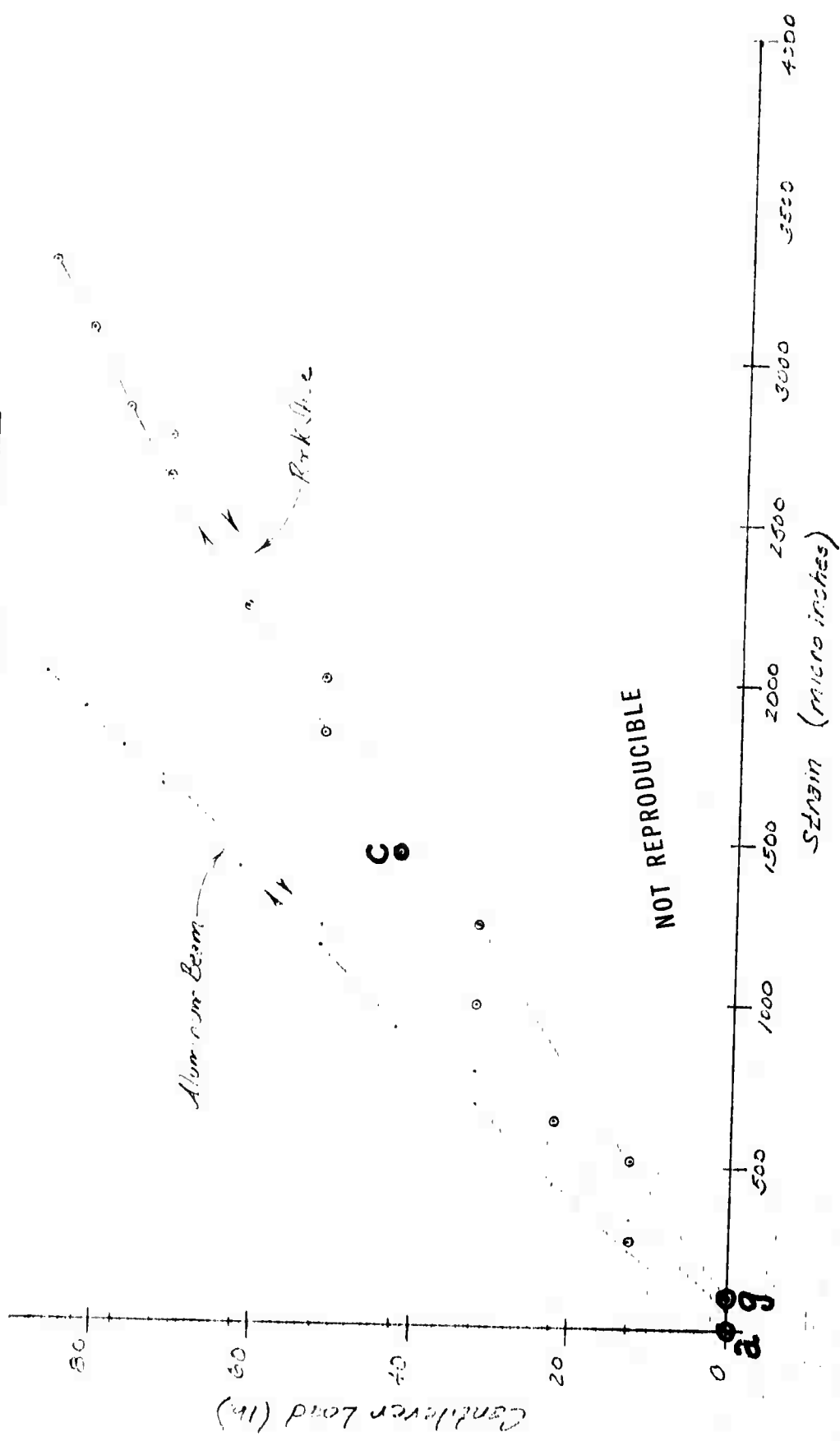
NOT REPRODUCIBLE



c

Figure 20 - Acetate peels made during deformation of a slice of Barre granite, face 1B. Load on the cantilever is toward the top of the pictures. Magnification = 4.4x. Inputs were masked to cover same area in each. a) b) and c) correspond to the points a, c, and g, respectively in Figure 21. Some fractures in a) appear to have widened and/or extended in b). New fractures appear in both b) and c). Some of those appearing in b) are longer in c).

LOADING CURVE TEST CENTRIFUGAL LOAD VS STRAIN



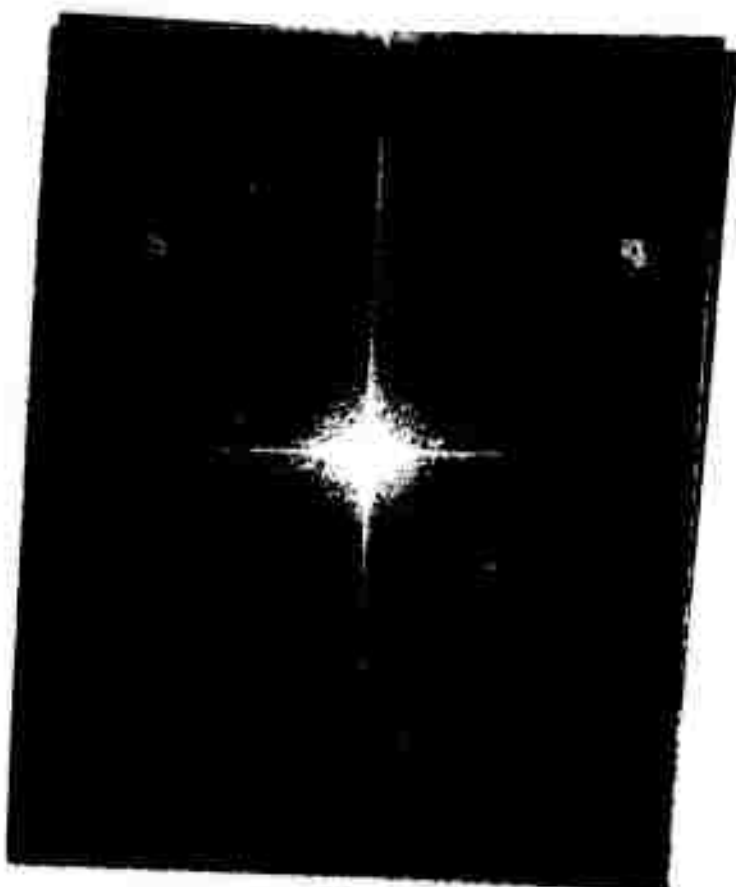
Scale:
 Vertical: 1lb./div.
 Horizontal: 25µin./div.

Test Identification No. C0016
 Sample I.D. No. E
 Rock Type Barr. Granite

Figure 21 - Loading curve for the deformation series illustrated in Figure 20.



a



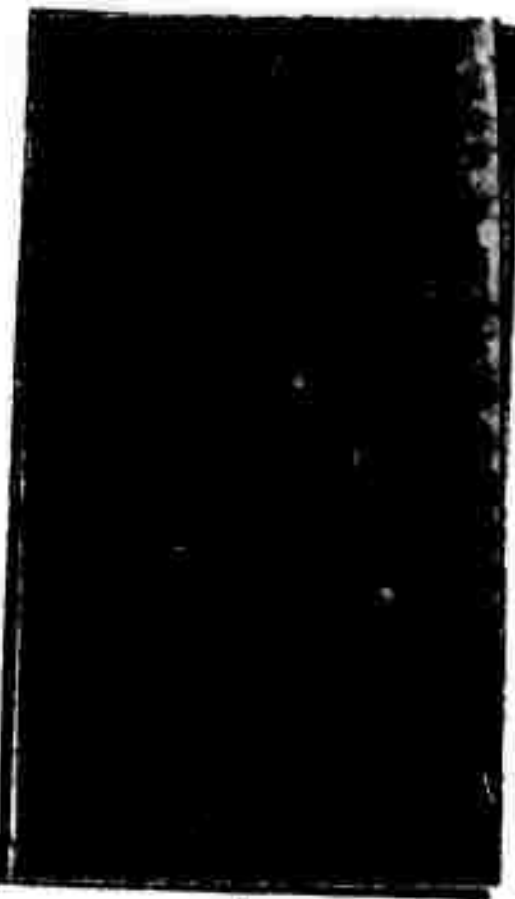
b



c

NOT REPRODUCIBLE

Figure 22 - Transforms corresponding to the inputs in Figure 21. Relative to a) there appear to be less high frequency and more low frequency elements in c). The diagonal stripe in b) is an artifact.



a



b



c

NOT REPRODUCIBLE



d



e

Figure 23 - Photographs showing axial deformation of a rectangular prism of Tennessee marble. Magnification 100x. (Courtesy of Dr. Syd Peng, U.S.G.M.)

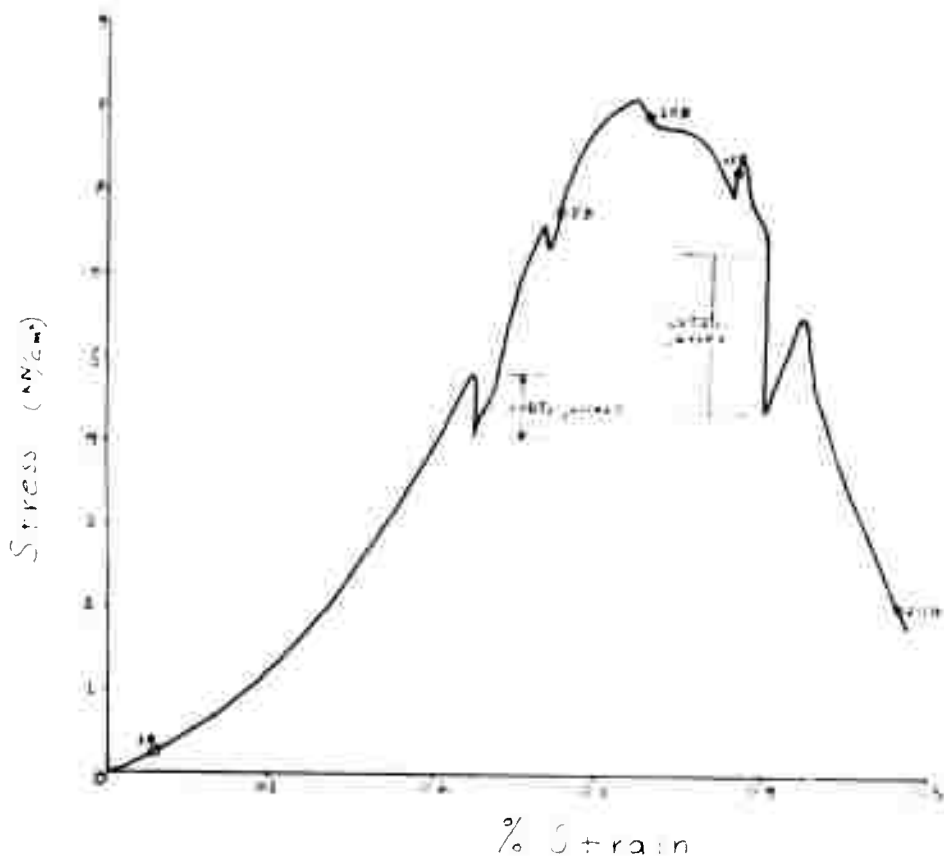
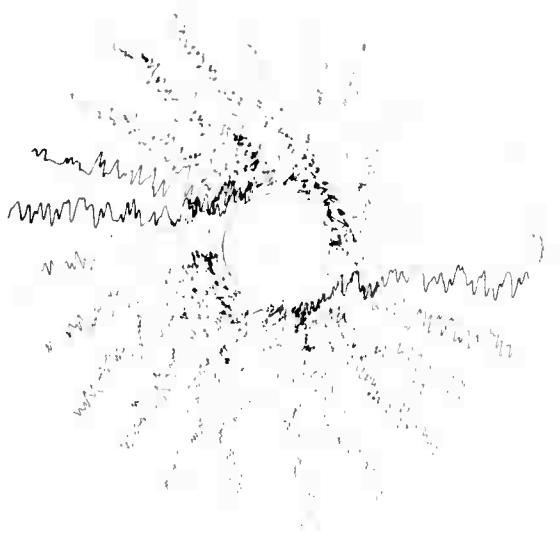


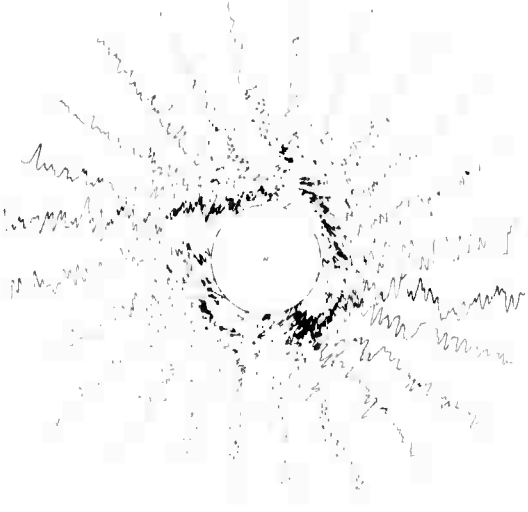
Figure 24 - Corrected stress/strain curve generated during the deformation experiment pictured in Figure 23. (Courtesy of Dr. Syd Feng, U.S.B.M.) Points 1B, 5B, 10B, 15B and 25B correspond to a, b, c, d, e, respectively in Figures 23 and 25.



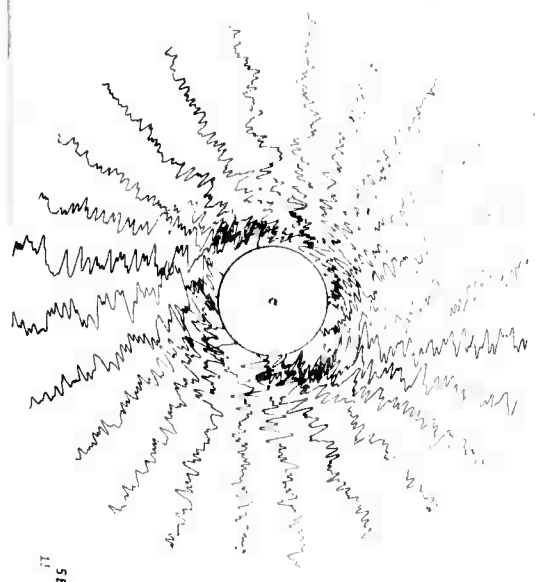
a



b



c

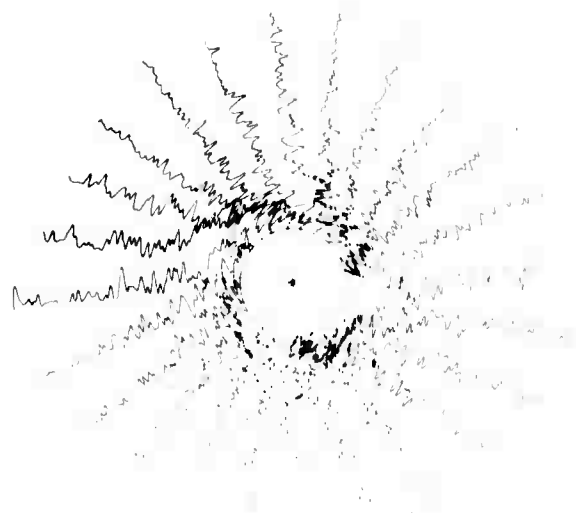


d

NOT REPRODUCIBLE



lines/cm.



e

Figure 26 - Maps of the transforms generated by the inputs pictured in Figure 23. c), d), and e) are oval with the major axis approximately horizontal. Rank in order of apparent decrease in spatial frequency: b), d) & e), a), c).

APPENDIX B

List of References Consulted

- Apostol, T. M., 1964, *Mathematical analysis*: Addison-Wesley, Reading, Mass.
- Atkins, K. R., 1965, *Physics*: J. Wiley and Sons, N. Y., 754 pp.
- Binns, R. A., Dickinson, A. & Watrasiewicz, B. M., 1968, Methods of increasing discrimination in optical filtering: *Applied Optics*, v. 7, no. 6, pp. 1047-1051.
- Billingsley, F. C., 1970, Applications of digital image processing: *Applied Optics*, v. 9, no. 2, pp. 289-299.
- Born, M. and Wolf, E., 1965, *Principles of optics*, 3d Ed.: Pergamon, N. Y., 808 pp.
- Bracewell, R. M., 1965, *The Fourier transform and its applications*: McGraw-Hill, New York, 381 pp.
- Bromley, K., Monahan, M. A., Bryant, J. F., and Thompson, B. J., 1971, Holographic subtraction: *Applied Optics*, v. 10, pp. 171-180.
- Brown, F. M., Hall, H. J., Kosar, J. (Eds.), 1966, *Photographic systems for engineers*: Soc. Phot. Sci. and Engrs., Washington, D. C., 215 pp.
- Cagnet, L. J., 1960, *An atlas of optical phenomena*: Prentice-Hall, Englewood Cliffs.
- Caulfield, H. J., & Lu, S., 1970, *The applications of holography*: Wiley-Interscience, New York, 138 pp.
- Cutrona, L. J., Leith, E. N. & Porcello, L. J., 1959, Filtering operations using coherent optics: *Proc. Nat. Electronics Conference*, pp. 262-275.
- Cutrona, L. J., Leith, E. N., Palermo, C. J., & Porcello, L. J., 1960, Optical data processing and filtering systems: *IRE Trans. Inf. Theory*, June, pp. 386-400.
- Davis, J. C., 1970, Optical processing of microporous fabrics: in *Data Processing in Biology and Geology*, J. L. Cutbill, ed. p. 69-87.
- Dobrin, M. B., Ingalls, A. L. and Long, J. A., 1965, Velocity and frequency filtering of seismic data using laser light: *Geophysics*, v. 30, pp. 1144-1178.
- Dobrin, M. B., 1968, Optical processing in the earth sciences: *I.E.E.E. Spectrum*, Sept. 68, pp. 59-66.
- Donath, F. A., Faill, R. T., and Tobin, D. G., 1971, Deformational mode fields in experimentally deformed rock: *Geol. Soc. Amer., Bull.*, v. 82, pp. 1441-1462.
- Dudderar, T. D., 1969, Applications of holography to fracture mechanics: *Soc. for Exper. Stress Anal.*, Paper No. 1451, 1969 Ann. Mtgs, 13 pp. + 7 Figs.
- Durelli, A. J. and Riley, W. F., 1965, *Introduction to photomechanics*: Prentice-Hall, New York, 402 pp.
- Esler, J. E., and Preston, F. W., 1967, Fortran IV program for the GE 625 to compute the power spectrum of geological surfaces: *Computer Contrib.* 16, Kansas State Geol. Surv., 23 pp.

- Fox, W. T., 1967, Fortran IV program for vector trend analyses of directional data: Computer Contrib. 11, Kansas State Geol. Surv., 36 pp.
- Francon, M., 1963, Modern applications of physical optics: Interscience, New York, 106 pp.
- Francon, M., 1966, Diffraction-coherence in optics: Pergamon Press, New York, 137 pp.
- Friedman, M., 1969, Petrofabric techniques for the determination of principal stress directions in rocks: Proc., Int. Conf. on State of Stress in the Earth's Crust, Elsevier, pp. 451-552.
- Gabor, D., Stroke, G. W., Brumm, D., Funkhouser, A., and Labeyrie, A., 1965, Reconstruction of phase objects by holography, Nature, v. 208, no. 5016, pp. 1159-1162.
- Gabor, D., Stroke, G. W., Restrict, R., Funkhouser, A., and Brumm, D., 1965, Optical image synthesis (complex amplitude addition and subtraction) by holographic Fourier transformation: Physics Letters, v. 18, no. 2, pp. 116-118.
- Grebowsky, G. V., 1970, Fourier transform representation of an ideal lens in coherent optical systems: NASA-TR-R-319, Washington, D. C., 62 pp.
- Green, A. E. and Adkins, J. E., 1970, Large elastic deformations: Clarendon Press, Oxford, 324 pp.
- Gresseth, E. W., 1964, Determination of principal stress directions through an analysis of rock joint and fracture orientations, Star Mine, Burke, Idaho, U. S. Bur. Mines Rept. Inv. 6413, 42 pp.
- Gresseth E. W. and Reid, R. R., 1968, A petrofabric study of tectonic and mining-induced deformations in a deep mine: U. S. Bur. Mines Rept. Inv. 7173, 64 pp.
- Harbaugh, J. W. and Sackin, M. J., 1967, Fortran IV program for harmonic trend analysis using double Fourier series and regularly gridded data for the GE 625 computer: Computer Contrib. 29, Kansas State Geol. Surv., 30 pp.
- Horino, F. G. and Ellickson, M. L., 1970, A method for estimating strength of rock containing planes of weakness: U. S. Bur. Mines Rept. Inv. 7449, 29 pp.
- Jackson, P. G., 1965, Analysis of variable density seismograms by means of optical diffraction: Geophysics, v. 30, pp. 5-23.
- Jaeger, J. C., 1962, Elasticity, fracture, and flow, with engineering and geological applications: 2nd Ed., Wiley, 152 pp.
- Jaeger, J. C. and Cook, N. G. W., 1969, Fundamentals of rock mechanics: Methuen, London, 513 pp.
- James, W. R., 1966, Fortran IV program using double Fourier series for surface fitting of irregularly spaced data: Computer Contrib. 5, Kansas State Geol. Surv., 19 pp.
- James, W. R., 1966, The Fourier series model in map analysis: Tech Rept. No. 1, ONR Task No. 388-078, Contract Nonr-1228(36), Geography Branch, O.N.R., 37 pp.

- Jenkins, R. W., 1969, Holographic optical data processing: NASA Tech. Memo. Rept. No. 53961, N70-17359, Marshall Space Flt. Ctr., Ala., 26 pp.
- Jennison, R. C., 1961, Fourier transforms and convolutions for the experimentalist: Pergamon Press, New York, 120 pp.
- Jeran, P. W. and Maskey, J. R., 1970, A computer program for the stereographic analysis of coal fractures and cleats: U. S. Bur. Mines, Info. Circ. 8454, 34 pp.
- Judd, W., 1969, Statistical methods to compile and correlate rock properties and preliminary results: ARPA Contract DACA 73-68-C-0002(P0002) Tech. Rept. No. 2, 109 pp.
- Kingslake, R., ed., 1967, Applied Optics and optical engineering: Academic Press, New York, vols. 1-5.
- Krumbein, W. W., 1966, A comparison of polynomial and Fourier models in map analysis: Tech. Rept. No. 2, ONR Task No. 388-078, Contract Nonr-1228(36), Geography Branch, O.N.R., 45 pp.
- Levi, L., 1968, Applied optics: John Wiley and Sons, New York.
- Lipson, S. G. and Lipson, H., 1969, Optical physics: Cambridge Univ. Press, Cambridge, 494 pp.
- Lurie, M., 1968, Fourier-transform holograms with partially coherent light: holographic measurement of spatial coherence: Jour. Opt. Soc. Amer., v. 58, no. 5, pp. 614-628.
- Markham, R., Frey, S. and Hills, G. J., 1963, Methods for the enhancement of image detail and accentuation of structure in electron microscopy: Virology, v. 20, pp. 88-102.
- Markham, R., Hitchborn, J. H., Hills, G. J., and Fred, S., 1964, The anatomy of the tobacco mosaic virus: Virology, v. 22, pp. 342-359.
- Merriam, D. F. and Harbaugh, J. W., 1969, Trend-surface analysis of regional and residual components of geologic structure in Kansas: Spec. Dist. Pub. 11, Kansas State Geol. Sur., 27 pp.
- Mitchel, R. H., 1969, Application of optical data processing techniques to geological imagery: Clearinghouse for Federal Scientific and Technical Information, Springfield, AD 695 120, 35 pp.
- Monahan, M. A., Bromley, K., Bryant, J. F. and Thompson, B. J., 1969, The use of holographic subtraction in the optical processing of reconnaissance data: NELC/ Report 1665, San Diego, 18 pp.
- O'Neill, E. L., 1963, Introduction to statistical optics: Addison-Wesley, Reading, Mass., 179 pp.
- Obert, L. A., and Duvall, W. I., 1967, Rock mechanics and the design of structures in rock: Wiley, 650 pp.
- Orhaug, J. and Svenssen, H., 1971, Optical processing for pattern properties: Photogrammetric Engrg., pp. 547-554.

- Overbey, W. K., Jr. and Rough, R. L., 1971, Prediction of oil - and gas-bearing rock fractures from surface structural features: U. S. Bur. Mines Rept. Inv. 7500, 14 pp.
- Parrent, G. B., Jr. and Thompson, B. J., 1969, Physical optics notebook: Soc. of Photo-optical Inst. Eng., Redondo Beach, Cal., 63 pp.
- Pennington, K. S. and Harper, J. S., 1970, Techniques for producing low-noise, improved efficiency holograms: Applied Optics, v. 9, pp. 1643-1650.
- Peterson, R. A., and Dobrin, M. B. (Eds.), 1966, A pictorial digital atlas: United Geophysical Corp., Pasadena, 53 pp.
- Pincus, H. J., 1966, Optical data processing of vectorial rock fabric data: Proc. First Int. Cong. on Rock Mechanics, v. 1, pp. 173-177.
- Pincus, H. J. and Dobrin, M. G., 1966, Optical processing of geological data: Jour. Geophys. Res., v. 71, no. 20, pp. 4861-4870.
- Pincus, H. J. and Ali, S., 1968, Optical data processing of multispectral photographs of sedimentary structures: Journal of Sedimentary Petrology, v. 38, no. 2, pp. 457-461.
- Pincus, H. J. and Gardner, R. D., 1968, Fluorescent dye penetrants applied to rock fractures: Int. J. Rock Mech. and Min. Sci., v. 5, no. 2, pp. 155-158.
- Pincus, H. J., 1969a, Sensitivity of optical data processing to changes in fabric- Part I-geometric patterns; Part II-standardized grain size patterns; Part III-rock fabrics: Int. Jour. Rock Mech. Min. Sci., v. 6, pp. 259-276.
- Pincus, H. J., 1969b, The analysis of remote sensing displays by optical diffraction: Proc., 6th Int. Symp. on Remote Sensing of Environment, U. Mich., V. 1, pp. 261-274.
- Pincus, H. J., 1970, The analysis of two-dimensional displays by optical diffraction with examples from the earth sciences: Proc., Electro-Optical Systems Design Conf., 1969, Industrial and Sci. Conf. Mgmt., pp. 625-632.
- Preston, F. W. and Harbaugh, J. W., 1965, BALGOL programs and geologic application for single and double Fourier series using IBM 7090/7094 computers: Spec. Dist. Pub. 24, Kansas State Geol. Surv., 72 pp.
- Ramsey, J. G., 1967, Folding and fracturing of rocks: McGraw-Hill, New York, 568 pp.
- Robinson, J. E., Charlesworth, H.A.K., and Kanasewich, E. R., 1968, Spatial filtering of structural contour maps: XXIII International Geol. Cong., v. 13, pp. 163-173.
- Rosenfeld, Azriel, 1969, Picture processing by computer: Academic Press, New York, 196 pp.
- Rosten, P., 1967, Image spectrum analyzer: A. F. Syst. Comm., Aerospace Rept. No. TR-1001 (2307)-17, A. F. Report No. SSD-TR-67-160, AD 663718, Los Angeles, 12 pp. + App. A-D.

- Sander, B., 1970, An introduction to the study of fabrics of geological bodies: Transl. by F. C. Phillips and G. Windsor, Pergamon, New York, 641 pp.
- Sherr, S., 1970, Fundamentals of display system design: Wiley-Interscience, New York, 484 pp.
- Shulman, A. R., 1970, Optical data processing: John Wiley & Sons, New York, 710 pp.
- Smith, H. M., 1969, Principles of holography: Wiley-Interscience, New York, 239 pp.
- Sommerfeld, Arnold, 1954, Lectures on theoretical physics, v. IV-Optics: Academic Press, New York, 383 pp.
- Stroke, G. W., 1966, An introduction to coherent optics and holography: Academic Press, New York, 358 pp.
- Tetelman, A. S. and McEvily, A. J., Jr., 1967, Fracture of structural materials: J. Wiley, New York, 697 pp.
- Tobin, D. G. and Donath, F. A., 1971, Microscopic criteria for defining deformational modes in rock: Geol. Soc. Amer., Bull., v. 82, pp. 1463-1476.
- Turner, F. J. and Weiss, L. E., 1963, Structural analysis of metamorphic tectonites: McGraw-Hill, New York, 545 pp.
- VanPelt, W. F., Stewart, H. F., Peterson, R. W., Roberts, A. M., and Worst, J. K., 1970, Laser fundamentals and experiments: BRH/SWRHL 70-1, U. S. Dept. of H. E. W., Govt. Printing Office, 117 pp.
- Vanderlugt, A., 1964, Signal detection by complex spatial filtering: IEEE Trans. Inf. Theory, IT-10, pp. 139-145.
- Vanderlugt, A., 1966, Practical considerations for the use of spatial carrier-frequency filters: App. Opt., v. 5, pp. 1760-1765.
- Vanderlugt, A., 1968, A review of optical data processing techniques: Optica Acta, v. 15, pp. 1-33.
- Vistelius, A. B., 1966, Structural diagrams: Transl. by R. Baker, transl. edited by N. L. Johnson and F. C. Phillips, Pergamon, New York, 178 pp.
- Wahlstrom, E. E., 1969, Optical crystallography: John Wiley & Sons, New York.
- Webb, R. H., 1969, Elementary wave optics: Academic Press, New York, 268 pp.
- Weinberger and Almi, 1971, Interference method for pattern comparison: Applied Optics, v. 10, pp. 2482-2487.
- Whitten, E. H. J., 1966, Structural geology of folded rocks: Rand McNally, Chicago, 663 pp.
- Willard, R. J. and McWilliams, J. R., 1969, Microstructural techniques in the study of physical properties of rock: Int. J. Rock Mech. Min. Sci., v. 6, pp. 1-12.
- Yu, F. T. S. and Bieringer, R. J., 1971, Optical correlation analysis of two-phase micrographs: Applied Optics, v. 10, p. 2269.

APPENDIX C

Outlines of Procedures

- I - Data sheet for specimens in uniaxial compression tests.
- II - Data sheet for specimens in rock slice tests: Cantilever (left) and third-part loading (right). Small square on rock slice is for photographic registration.
- III - Data sheet for loading experiments.
- IV - Orientation code for specimens cut from rock cubes of known orientation.
- V - Photograph identification code.
- VI - Summary of film characteristics for optical data processing, as observed by this project's personnel.
- VII - Procedure for reversal development (Figure 15).
- VIII - Procedure for photographing with telemicroscope.
- IX - List of available photographic equipment.
- X - Procedure for mapping transforms.
- XI - Types and sizes of filters (Film and glass).
- XII - Log of inputs and outputs for optical diffraction analysis.
- XIII - Optical diffraction processing log.
- XIV - Scanning log for mapping transforms.
- XV - Acetate sheet peel technique for rock slices.
- XVI - Procedure for holographic subtraction.

I - Data sheet for specimens in uniaxial compression tests.

FORM 1 - Uniaxial Compression Tests

C-2

Test Identification No. _____

Sample Identification No. _____

Operator _____

Date _____

Strain Gage Data

Resistance

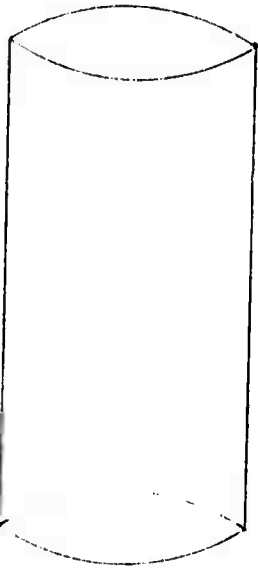
Gage Factor

F_{box}

K

Temperature Compensation

Specimen Dimensions and Gage Locations



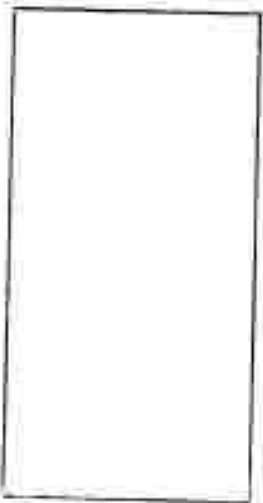
Average Diameter: _____
Two orthogonal readings measured at mid-height.

Average Length: _____
Three equally spaced readings using calipers.

End Variation: _____

Accuracy: Length and Diameter measurements to nearest 0.01, End Variation to 0.001.

Comments



II - Data sheet for specimens in rock slice tests: Cantilever (left) and third-part loading (right). Small square on rock slice is for photographic registration.

FORM 2 - Rock Slice Tests

C-3

Test Identification No. _____

Sample Identification No. _____

Operator _____

Date _____

Strain Gage Data

Resistance

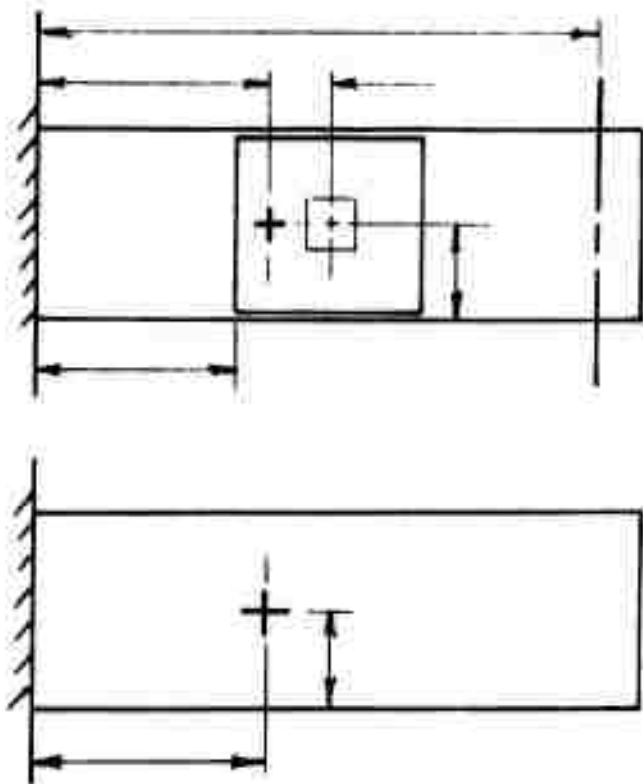
Gage Factor

F_{box}

K

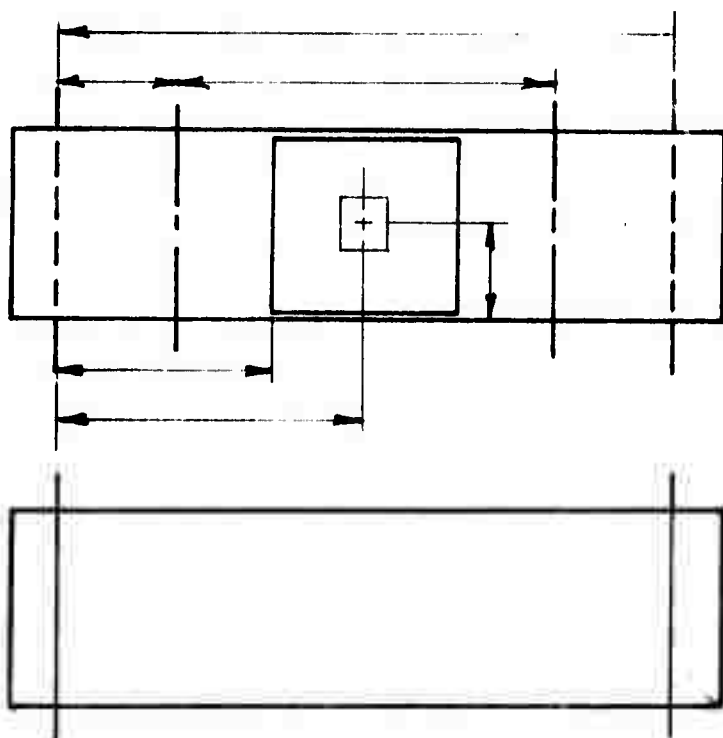
Temperature Compensation

Specimen Dimensions and Orientation and Gage Location



Top Views

Bottom Views

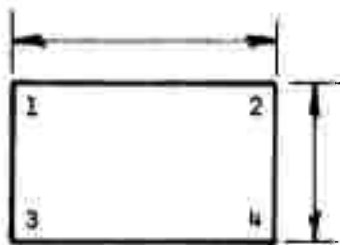


Cantilever Loading Apparatus

Three-Part Loading Apparatus

Rock Slice Thickness Data:

Comments:



1 2 3 4

Rock
Total
Epoxy

The purpose of the orientation code is to define the orientation of the specimen with respect to the "orientation" or "north" arrow on the cubic rock sample.

Six principal faces of the cube, "1", "1B", "2", "2B", "3" and "3B", are defined in the following manner:

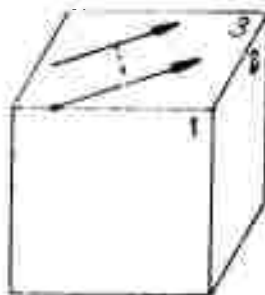
Face 3 is the "top" of the block on which the north or orientation arrow is located.

Face 1 is determined by moving the north or orientation arrow laterally until the base of the arrow is on an edge of the cube and the arrow is pointing normal or up and to the right from the edge. The face which the base of the arrow intersects is face 1.

Face 2 is counterclockwise from face 1 and adjacent to face 1 and face 3.

Face 1B, 2B and 3B, are the corresponding parallel faces opposite to faces 1, 2, and 3, respectively.

The foregoing definitions are applied to the illustrated sample cube:

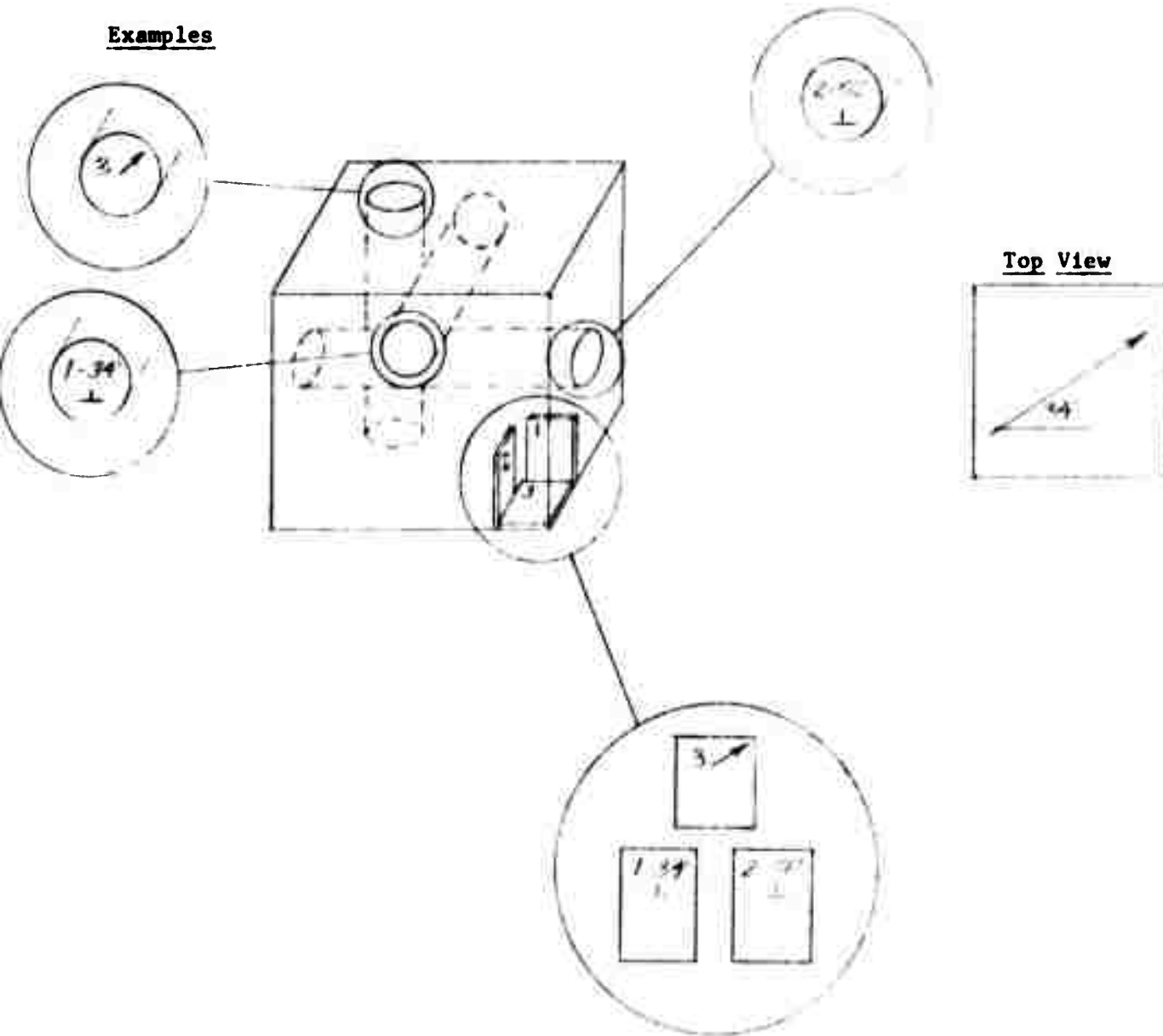


The research, at this time, will require specimens cut from the block in three mutually perpendicular directions. These directions correspond to the axes which are perpendicular to one of the six cube faces previously defined.

A core or slice cut from the cube is denoted by three symbols:

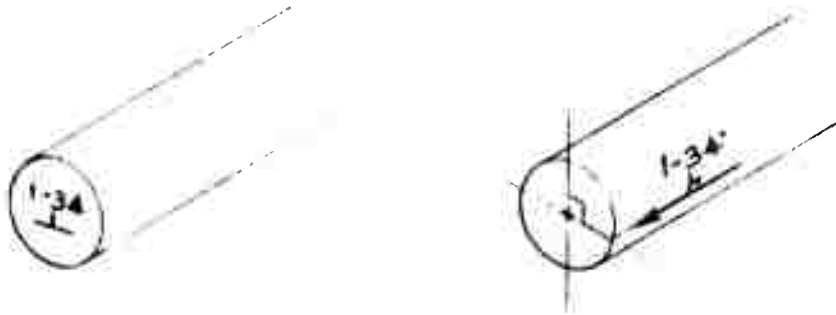
- (1) A number denoting the face of the cube which the specimen contains, ie., 1, 1B, 2, 2B, 3 or 3B.
- (2) An acute or right angle specifying the number of degrees the orientation or north arrow makes with the face under consideration.
- (3) A horizontal indicator symbol for elements cut horizontally from faces 1, 1B, 2, or 2B.

Examples

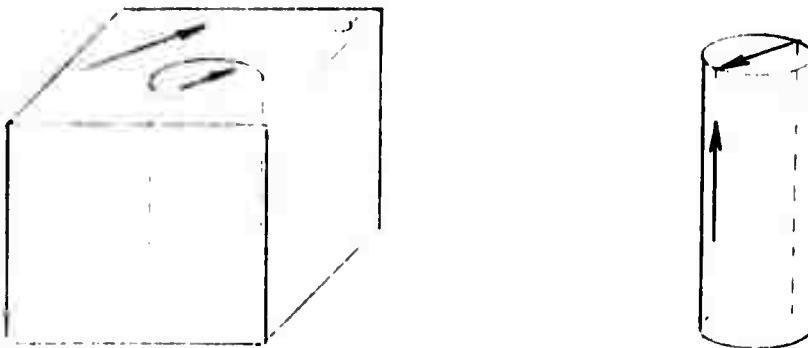


Since the machining operations for specimen preparation will eradicate any orientation markings on the machined ends or surfaces, the orientation must be transferred to another surface.

For cylindrical cores cut from faces 1, 1B, 2, or 2B, the orientation symbols are transferred from the end of the core to its side as shown on the following page.



For cylindrical cores cut from face 3 and 3B, the orientation line is transferred as follows:



After machining the orientation arrow can be re-established on the end of the core.

The same procedure may be adopted in principle for the rock slices. Extreme care must be exercised by the machinist to avoid errors.

This code may be expanded, when needed, to include cuts made at angles other than 90 degrees to the cube faces.

First Four Digits - identification of test

First Digit- capital letter indicating type of test

- C = cantilever weight loaded
- C₁ = cantilever micrometer loaded
- P = third-part loading
- U = uniaxial loading

Second Digit- a numeral

Third Digit - a numeral

Fourth Digit - a numeral

Fifth Digit - location of photograph within a test
a small letter

Sixth - Ninth Digits - sample identification

Sixth Digit - capital letter indicating general rock type

- A = acid igneous
- B = basic igneous
- I = intermediate igneous
- S = sandstone
- L = limestone
- D = dolomite
- M = shale, mudstone
- C = conglomerate
- F = foliated or lineated metamorphic
- G = nondirectional structure metamorphic

Seventh Digit - a numeral

Eighth Digit - a numeral

Ninth Digit - a numeral

Tenth Digit - test equipment orientation relative to dimensions of negative, L if bar long direction parallels long direction of negative; W if it parallels short direction for U test, L if axis connecting platens parallels long direction of negative; W if axis parallels the short direction

Eleventh and Twelfth Digits - feature orientation, the angle of the feature with the long direction of the negative, two numerals

Thirteenth Digit - a symbol for any additional information

Summary of film characteristics for optical data processing, as observed by this project's personnel.

Film Type	Inputs	Outputs	Filters	Remarks
Panatomic-X	Excellent resolution and graininess acceptable	Too slow	Lack of contrast makes it unacceptable. May be useful if reversal developed.	Will try to develop to a higher ASA, and then use with the Kesselblad.
Plus-X Pan	Except for lower resolution, the same as Panatomic-X	Preferred over Panatomic-X only because of its higher speed	Same as Panatomic-X	Excellent for reversal development
Tri-X Pan	Too grainy	Too grainy	Too grainy	
High-contrast Copy	Excellent for black-white with no gray tones.	Unacceptable because of filtering effect of high contrast film.	Can be used to record binary filters.	Difficult ASA to work with. Thin base - in lead in instability in gate
Agfa-Gaerort 10E75	Same as High Contrast Copy but much higher resolution. Relatively expensive.	Excellent results in holography. Only fair for transfers. Slow	Excellent results for all but the finest half-tone patterns. Post mechanical stability in film used.	Film has thin base. Plates very expensive. Will try high resolution developer in future
Kodak Projector Slide Plates	Unacceptable due to irregularities in the emulsion.	Same as high contrast copy.	Very good results. Mechanically stable.	
Polaroid films	Wasteful format - expensive	Excellent for monitoring purposes	Not tried	NOT REPRODUCIBLE
Super-X Pan type 4142	Wasteful format	Excellent for many filtered reconstructed images and high frequency transfers	Not tried	
Kodalith	Same as high contrast copy but higher contrast	Same as high contrast copy	Same as high contrast copy but higher contrast	Many "pinholes" in the emulsion need to be painted out.

VII - Procedure for reversal development (Figure 15)

Most successfully applied to Plus X Pan. The film is exposed according to usual procedure (i.e., ASA 125). Development in general (modified from Howard, 1971):

- i) 4 min Kodak D-19.
- ii) 1 min. wash in warm water - this must be thorough; not just filling the container and letting it sit.
- iii) 2 min. bleach R-9 - must be fresh.
- iv) 1 min. wash (note above).
- v) 1 min. clear CB.
- vi) 1 min. wash.
- vii) reexposure: the film is laid emulsion side up on a bench so that no shadows are cast upon it when the overhead lights are turned on for 15-30 seconds. This gives a uniform illumination.
- viii) 2-4 min. Kodak D-9.
- ix) 30 sec. Kodak stop or indicator stop bath.
- x) 1-2 min. Kodak rapid fix.
- xi) 5 min. wash.

*carried out in total darkness

Agitate 5 sec. in 15. (Figure 15 contains a diagrammatic representation of the process.)

VIII - Procedure for photography with telemicroscope.

Equipment

Telemicroscope; Accura T Fitting; Aetna T mount Microscope adapter; tripods, 3200 K flood lights; Plus-X Pan Film; Graph Paper; Prontor Cable Release; Camera Body either Practina or Pentax.

Procedure

- Step 1. Place specimen in position.
- Step 2. Mount the telemicroscope on its support (tripod).
- Step 3. Remove ocular from telemicroscope.
- Step 4. Clamp on the microscope that portion of the microscope adapter that fits on the microscope barrel.
- Step 5. Replace the ocular in the telemicroscope.
- Step 6. Place the barrel portion of the microscope adapter on the camera body (use the accura T fitting for the Practina. For the Pentax screw the barrel onto the camera body until resistance is felt; do NOT use any force in this operation for this will result in stripping the threads.)
- Step 7. Now attach the camera to the telemicroscope by matching the red dots on the adapters and then turning the camera portion clockwise.
- Step 8. Release the clamp and turn the entire adapter assembly and the camera until it is in the desired orientation, and tighten the clamp.
- Step 9. Unless the telemicroscope assembly is in a vertical orientation the camera body must now be supported by another tripod.
- Step 10. Attach the Prontor Cable release to the camera.
- Step 11. Cock the Camera shutter.
- Step 12. Focus on the specimen by doing the following: Place a piece of graph paper on the specimen. Turn on the flood lights. Focus by turning the knob on the microscope or by adjusting the focus on the lens or by a combination of both. Note: When the knob on the microscope is turned the camera must move, thus the clamps on the camera's tripod must be loose.
- Step 13. Set shutter speed at B.
- Step 14. Lens should be set with f-stop wide open.
- Step 15. Initially, take pictures of the specimen and the graph paper at times of 2, 3 and 4 seconds.

IX - List of available photographic equipment

- * 1. Practina 35mm SLR.
 2. Speed graphic view camera.
 3. Calumet view camera.
 - * 4. Hasselblad 500 with standard and wide angle lenses, bellows, light shield.
 5. Bausch and Lomb/Nikon 135mm telemicroscope.
 6. Polaroid photomicrography set-up.
 7. Practina adapters for microscope.
 8. Bownes Illumitran and accessories.
 9. Exakta 35mm SLR.
 10. Polaroid 46-L back for view cameras.
 11. 120 back for view cameras.
 12. Polaroid 4x5 (52, 55, 57) back for view cameras.
 - ** 13. Nikon F 35mm SLR and accessories.
 - ** 14. Pentax 35mm SLR and accessories.
 - ** 15. Minolta 25mm SLR and accessories.
- * adapted to optical diffraction analysis.
- ** available if needed.

X - Procedure for mapping transforms.

The basic scanning hardware is a prototype unit purchased from Conduction Corp. and consists of:

- 1) Scanner: a photomultiplier tube completely enclosed except for a pinhole towards the laser and at the height of the system's optic axis. The size of the pinhole can be varied. The photomultiplier can be translated horizontally, orthogonal to the optical axis. The entire assembly can be readily secured to the bed of the optical bench.
- 2) Photomultiplier power supply: Harrison 6515A DC power supply manufactured by Hewlett-Packard.
- 3) Ammeter: #414 micro-micro ammeter manufactured by Keithley Instruments.

The output from the ammeter can be fed into any X-Y plotter or strip chart recorder with a variable time base in order to record individual scans across a transform.

The phototransparency X-Y- θ input gate is manufactured by Ardel Corp. It consists of two TT-100 translation modules to provide X-Y movement and one KT-175, 360° rotatable module to provide rotation about the optic axis. The stacked modules are mounted with a #775 post, an #10 base and a #77 adapter.

The input assembly was modified by the insertion of pins at 90° intervals around the circular opening of the KT-175. These are used for securing the input to the gate. A set screw was also added in order to eliminate rotation about the vertical mounting rod.

General mapping procedure

1. Before the bench is converted to the mapping configuration pictures of the transform to be mapped and a corresponding calibration transform must be recorded.
2. The highest desired resolution frequency is determined from the pictures of the transform.
3. From the time base constants of the recorder and the velocity of the scanner, a maximum "half-transform distance" is determined and the scanner is positioned accordingly.
4. The input gate is placed on the optical bench in its proper position to ensure its orthogonality with the optic axis.
5. Square tape is used to mark one of two thick optical flats so that when the input is placed on it only the desired rectangular portion of the input will be illuminated.
6. The calibration grid is sandwiched between the two glass flats and mounted on the X-Y- θ input gate. The marked aperture is centered on the optic axis.

7. The viewing microscope is focused on the transform generated by the input in the first transform plane and, using a horizontal knife edge filter, the rotary gate is adjusted so that one arm of the cross generated by the rectangular aperture is parallel to the knife-edge filter.
8. The transform enlarging lens is placed on the bench so that the second transform is approximately focused in the plane of the scanner pinhole.
9. A beam splitter and a telemicroscope (or whatever will do) are used to observe the plane of the scanner pinhole and the transform is focused by adjusting the frequency enlarging lens.
10. The X-Y adjustments on the frequency enlarging lens and the scanner micrometer are used to center the transform, by obtaining a maximum reading on the ammeter.
11. The scanner is translated one-half transform width and is scanned towards the transform center several times while adjusting the voltage controls of the plotter and those of the ammeter so that the maximum intensity of the DC spot is recorded almost full scale.
12. A full scan of the calibration transform is recorded and compared with the maximum resolvable frequency desired. If unsatisfactory, the position of the scanner is readjusted, and then proceed from step #9.
13. After obtaining a satisfactory calibration scan, the first input is inserted, as per steps #6 to #10, and then scanned.
14. The input is rotated through the desired number of degrees, centered and scanned again.
15. The scans are plotted radially in proper orientation using the DC spot as a centering guide.

All measurements in millimeters.

- #1. Low-cut frequency filters
 Center=0.35
 Outside diameters=0.7, 0.8, 1.0, 1.15, 1.3, 1.5, 1.65,
 1.8, 1.95, 2.1, 2.3, 2.45, 2.6, 2.8
- #2. Band-cut filters
 All are 0.7 mm thick
 Outside diameters=2.95, 3.1, 3.3, 3.5, 3.65, 3.8
- #3. Band-cut filters
 All are 0.7 mm thick
 Outside diameters=1.4, 1.6, 1.8, 2.0, 2.2, 2.35, 2.55,
 2.75
- #4. High-cut or band-cut filters
 Outside diameters=3.35 mm on all filters
 Inside diameters=0.95, 1.1, 1.3, 1.6, 1.9, 2.3, 2.6,
 2.9
- #5. Band-pass filters with dc block
 Measurements the same as in #2
- #6. High-cut filters with dc block
 Measurements the same as in #1
- #7. Band-pass filters with dc block
 Measurements the same as in #3
- #8. Band-pass or low-cut filters with dc block
 Measurements the same as in #4
- #9. Band-cut ellipses
 Lead: outside-inside minor axes X outside-inside major axes.
 1.2-1.2 X 4.2-3.0, 2.4-1.7 X 3.95-3.0, 2.8-2.1 X 3.9-2.9,
 1.2-0.7 X 3.9-1.7, 2.35-1.0 X 3.9-1.8, 2.8-1.2 X 3.9-1.6,
 1.2-1.1 X 4.0-2.6, 2.4-1.5 X 3.95-2.6, 2.25-1.8 X 4.0-2.6,
 1.2-1.1 X 4.0-1.4, 2.3-0.8 X 3.9-1.4, 2.8-1.0 X 3.9-1.4
- #10. Band-cut ellipses
 Lead: outside-inside minor axes X outside-inside major axes.
 0.95-0.55 X 1.9-1.25, 0.95-0.75 X 1.9-1.25, 1.4-0.9 X 1.9-1.25,
 0.9-0.55 X 1.9-0.7, 1.15-0.4 X 1.9-0.7, 1.4-0.5 X 1.9-0.7,
 0.9-0.55 X 1.9-1.45, 1.2-0.85 X 1.9-1.45, 1.4-1.0 X 1.9-1.45,
 0.9-0.55 X 1.9-0.9, 1.15-0.55 X 1.9-0.9, 1.4-0.65 X 1.9-0.9

NOT REPRODUCIBLE

- #11. Band-cut ellipses
Read: as in #9.
0.75-0.25 X 1.0-0.35, 0.6-0.2 X 1.0-0.35, 0.5-0.1 X 1.0-0.35,
0.75-0.45 X 1.0-0.6, 0.65-0.35 X 1.0-0.6, 0.5-0.25 X 1.0-0.6,
0.75-0.3 X 1.0-0.45, 0.65-0.25 X 1.0-0.45, 0.5-0.2 X 1.0-0.45,
0.75-0.55 X 1.0-0.75, 0.65-0.4 X 1.0-0.75, 0.5-0.35 X 1.0-0.75,
- #12. Concentric circles and ellipses
Circle: 4.4 to 0.25 mm. in diameter
Ellipse: 2.8-0.4 X 4.C-0.65
- #13. Band-pass ellipses with dc block
Measurements the same as in #9
- #14. Band-pass ellipses with dc block
Measurements the same as in #10
- #15. Band-pass ellipses with dc block
Measurements the same as in #11
- #16. Concentric circles and ellipses with dc block
Measurements the same as in #12

In addition, filters have been constructed using the following as targets. Data on filter measurements are not available at this time. All of these filters are on film. A few glass copies have been prepared.

Procedure: The spatial filters were constructed on $8\frac{1}{2}$ x 11 sheets of white paper.

The following is a list of the filters constructed:

1. Solid black circle with 1" radius.
2. Solid black ring (2" radius, 1" inner radius) with black circle $\frac{1}{4}$ " diameter in center.
3. Solid black cross 5 mm wide.
4. Cross 5 mm wide, Letratone pattern #100.
5. Pairs of wedges with $40^\circ \angle$, Letratone pattern # 57, 61, 63, 97, 98, 99, 100, 936.
6. Rings, outer radius 2", 1" inner radius, Letratone pattern #57, 61, 63, 97, 98, 99, 100, 936.
7. Black ring (2" outer radius, 1" inner radius) bounded on inside and outside by rings (5 mm radius) of Letratone pattern # 57, 61, 63.
8. Black ring (2" outer radius, 1" inner radius) bounded on inside and outside by rings (1/8" radius) of Letratone pattern # 97, 98, 99, 100.
9. Pair of solid black wedges ($40^\circ \angle$) bounded on sides by shading of 50 each of patterns # 97, 98, 99, 100.

10. Pair of solid black wedges (40°) bounded on sides by 6 mm wide strips of Letratone pattern # 57, 59, 61, 63.
11. Pair of solid black wedges (40°) bounded on sides by 6 mm wide strips of Letratone pattern # 97, 98, 99, 100.
12. Strip composed of 1" squares of Letratone pattern # 57, 61, 63.
13. Strip composed of 1" x $\frac{1}{2}$ " rectangles of Letratone pattern # 57, 61, 63.
14. Strip composed of 1" squares of Letratone pattern # 97, 98, 99, 100.
15. Strip composed of 1" x $\frac{1}{2}$ " rectangles of Letratone pattern # 97, 98, 99, 100.
16. Strip 9" x 1", Letratone pattern #87.
17. Strip 9" x $\frac{1}{2}$ ", Letratone pattern #87.

Log of Inputs and Outputs

(Date) _____

(Entered by) _____

(Log Sheet No.) _____

Input Source and Description _____

Input Processing:

<u>Input Serial No.</u>	<u>Reduction</u>	<u>P. or N.</u>	<u>Best Frame(s)</u>	<u>Remarks</u>
-------------------------	------------------	-----------------	----------------------	----------------

Outputs:

<u>Output Serial No.</u>	<u>OPP Operation</u>	<u>Ref. Lab Sheet Nos.</u>	<u>Remarks</u>
--------------------------	----------------------	----------------------------	----------------

NOT REPRODUCIBLE

17. Arrange sheet just beneath the rock above.

Procedure:

1. Arrange.
2. Roll sheet under stone.
3. Close sample with surface under edge of specimen.
4. Roll sheet under just a little longer than sample.
5. Apply pressure so that it covers entire surface.
 - a. Notice separation rate.
 - b. Notice where the system accumulated on the surface.
6. Apply pressure covering entire surface.
7. After 1 or 2 sec. apply sheet close to the surface.
 - a. If sheet is curled, place it so that it curls toward the sample.
 - b. Place sheet so that it contacts the part of the surface where the system accumulated first.
 - c. Slowly roll the sheet so that it contacts the rest of the surface.
 - d. Allow to set for several seconds.
8. Apply gentle pressure with fingers to center of the surface and work the fingers out to the edges in order to remove air bubbles.
9. Allow to dry for 5 minutes.
10. Remove gel from surface with a slow gentle peeling motion from one side of the surface to the other side.
11. Place gel between flat surfaces and apply pressure to prevent curling of the gel for about one hour.
12. Flatten one side of gel by placing them between glass plates and cooling edges.

IV - Procedure for holographic subtraction.

1. Produce the desired hologram.
2. Adjust the optics behind the hologram so that the original input can be monitored via the closed circuit television system.
3. Replace the developed hologram in the position in which it was recorded.
4. Precisely realign the hologram by viewing it through the microscope and adjusting the relative positions of the transform and hologram; realignment is complete when no laser light can be seen in the recording plane.
5. There should now be little if anything to view on the television monitor; if there is still some of the image visible adjust the relative transform/hologram positions to achieve complete subtraction. This appears as one large black fringe over the entire input whereas partial subtraction appears as a smaller fringe or fringes. If the image appears reinforced the optical configuration used to record the hologram has probably been altered and a fresh start would be advised.
6. Replace the first input with one of those from which it is to be subtracted.
7. Two images will probably be visible on the monitor; one is the input and the other is generated by the hologram. Adjust the input so that the images overlap in their proper orientations with respect to each other.
8. Replace the vidicon with a camera and record the difference between the two inputs.